SECTION III

PUBLISHED PAPERS

IN

JOURNALS

AND

CONFERENCE PROCEEDINGS

(JULY 1981-JUNE 1982)

Diffractive Excitation in Quantum Chromodynamics

G. Bertsch,[a] S. J. Brodsky,[b] A. S. Goldhaber,[c] and J. G. Gunion[d]
Institute for Theoretical Physics, University of California, Santa Barbara, California 93106
(Received 11 May 1981)

Hadronic collision models based on quantum chromodynamics predict remarkably large cross sections for diffractive scattering of hadrons on a nuclear target. The diffraction arises from the transparency of a nucleus to the portion of the projectile wave function having small transverse separation between its constituents. Correspondingly, the typical transverse momentum within the diffracted system is significantly enhanced. This quantum-chromodynamics–based picture leads to large cross sections for diffractive charm production.

PACS numbers: 13.85.Hd, 12.40.Cc, 24.90.+d

Diffractive dissociation, as explained in the classic papers of Feinberg and Pomeranchuk[1] and of Good and Walker,[2] is a distinctive quantum effect which makes up a significant part of the total hadron-hadron cross section at high energy. In a typical dissociation event, the target recoils intact with small momentum transfer, while the projectile is excited to a state with constituents having low transverse momentum. The diffractive excitation arises from the variability of the absorption amplitude as a function of the internal coordinates of the projectile wave function. We wish to focus attention on the enhanced possibility of studying hadronic wave functions by diffractive dissociation on nuclear targets. In a quantum-chromodynamics–based picture of hadron-hadron total cross sections,[3,4] the components of a color-singlet projectile wave function with small transverse separation pass freely through the nucleus while the large-transverse-separation components are nearly totally absorbed.[5] In short, a large target will act as a filter, removing from the beam all but the short-range components of the projectile wave function. The cross section for diffractive production of inelastic states is then equal to the elastic scattering cross section of the projectile on the target, multiplied by the probability that sufficiently small transverse separation configurations are present in the wave function.

The relevant portions of the wave function can be calculated in quantum chromodynamics (QCD), because the short-distance behavior is in the perturbative domain.[6,7] The QCD wave function is represented in terms of Fock components defined at equal time on the light cone; internal coordinates are the transverse position $r_{\perp i}$ and the light-cone momentum fraction $x_i = (k_0 + k_3)_i/(p_0 + p_3)$ of each constituent, where p is the projectile momentum in a frame with $p^1 = p^2 = 0$. For the interaction between hadrons we make use of the gluon-exchange model of Low and Nussinov.[3] An immediate consequence[4] of the model is that the interaction depends strongly on the configuration of the constituents of the hadron. For Fock components with many constituents, it is very improbable for all the transverse separations to be small. Only the valence Fock configuration has a wave function $\xi(x, r_\perp)$ which is large as $r_\perp \to 0$,[6,7] and hence a wave-function component which is totally noninteracting.[8]

At high energy the S matrix may be written as a function of impact parameter b, and internal projectile coordinates $\xi = (x_i, r_{\perp i})$. The projectile wave function ψ is normalized, $\int d\xi\, |\psi(\xi)|^2 = 1$. After filtering by the target, the surviving hadron wave function is

$$S(b,\xi)\psi(\xi) = \psi'(b,\xi). \tag{1}$$

Defining $\bar{S}(b) = \int d\xi\, |\psi(\xi)|^2 S(b,\xi)$, the expectation value of S for the incoming hadron, we decompose ψ' as

$$\psi'(b,\xi) = \bar{S}(b)\psi(\xi) + [S(b,\xi) - \bar{S}(b)]\psi(\xi). \tag{2}$$

The first term is simply the survival amplitude of the incident state, while the second term is a superposition of excited hadron states orthogonal to the incident state. If for certain values of ξ there is weak absorption, $S(b,\xi) \simeq 1$, then the cross section for producing such ξ's is given by

$$d\sigma/d\xi = \int d^2b\, |1 - \bar{S}(b)|^2 |\psi(\xi)|^2 = \sigma_{el} |\psi(\xi)|^2, \tag{3}$$

where σ_{el} is the elastic scattering cross section. Thus the diffractive cross-section ratio $(\sigma_{el})^{-1} \times d\sigma/d\xi$ directly measures the original wave function.

As an example, consider a pion projectile. We treat the interaction of the $q\bar{q}$ Fock component, and assume that the higher Fock components are completely absorbed. The asymptotic form of

Limit on Charge Symmetry Breaking in the Optical Model and the Coulomb-Energy Anomaly

R. P. DeVito,[a] Sam M. Austin, W. Sterrenburg,[b] and U. E. P. Berg[c]
Cyclotron Laboratory and Physics Department, Michigan State University, East Lansing, Michigan 48824

(Received 9 March 1981)

Cross sections for elastic scattering of neutrons from ^{40}Ca have been measured at 30.3 and 40.0 MeV and analyzed to obtain optical-model potentials. The optical potentials for neutron and proton scattering are found to be very similar after a correction for Coulomb effects, indicating that a static charge-symmetry-breaking Hartree potential is too small to explain the Coulomb-energy anomaly for bound states.

PACS numbers: 25.40.Dn, 21.10.Dr, 24.10:Ht

At first glance it seems that it should be simple to calculate the difference in the masses of two mirror nuclei such as ^{3}H and ^{3}He or ^{41}Ca and ^{41}Sc. That simple approaches fail, by more than 500 keV in the case of the ^{41}Ca-^{41}Sc pair, was first pointed out by Nolen and Schiffer[1] and this difference became known as the Coulomb-energy or Nolen-Schiffer anomaly. In spite of an intense theoretical effort since this discovery,[2] and the calculation of many small (and mostly canceling) corrections, the problem remains. In a survey of the situation, Negele[3] concluded that the only apparent solution was to introduce a small charge-symmetry-breaking (CSB) potential in the nucleon-nucleon interaction, such that the strong interaction between two neutrons (V^{nn}) is more attractive than that between two protons (V^{pp}). As a result, the extra neutron in ^{41}Ca is bound more tightly than the proton in ^{41}Sc, reducing the discrepancy. In a schematic Hartree model, Negele showed that a difference of about 20 MeV fm^3 in the volume integrals of V^{pp} and V^{nn} is sufficient to remove the anomaly. A difference of this size is not predicted by the usual theoretical models[2,4] but is consistent with experimental determinations of the scattering lengths and effective ranges for the nn and pp systems.[4]

Of course, a charge-symmetry-breaking potential such as that proposed by Negele[3] will affect not only the potential felt by bound nucleons, but also the optical-model potential describing nucleon scattering. In this Letter we describe a measurement of elastic scattering from ^{40}Ca at 30.3 and 40.0 MeV. With these results, neutron scattering data are available over a sufficiently large energy range to permit a rather precise comparison with the available proton scattering data. We have obtained optical-model potentials for the neutron data and have compared the real parts of these potentials with those for protons. After a correction for Coulomb effects, the neutron and proton potentials are nearly the same, with the result that a CSB Hartree potential of the sort originally discussed by Negele[3] seems implausible. This appears to be the first sufficiently sensitive test of Negele's conjecture, although the reliability of the optical model for this purpose needs further investigation.

The experiments were performed with use of the Michigan State University beam swinger time-of-flight system, as adapted for neutron scattering.[5] Neutrons produced by the reaction ^{7}Li(p, n)^{7}Be were scattered from encapsulated cylindrical targets of natural metallic calcium[6] and were detected with an overall resolution of 0.75 to 1.4 MeV by a liquid-scintillation detector placed 5–9 m from the scatterer. Backgrounds from the thin aluminum container and from air scattering were

Higher-Order Deformations of ^{232}Th and ^{234,236,238}U

R. M. Ronningen, R. C. Melin,[a] J. A. Nolen, Jr., and G. M. Crawley
Physics Department and Cyclotron Laboratory, Michigan State University, East Lansing, Michigan 48824

and

C. E. Bemis, Jr.
Physics Division, Oak Ridge National Laboratory, Oak Ridge, Tennessee 37830

(Received 10 July 1981)

We have measured the inelastic scattering of 35-MeV protons from ^{232}Th and from ^{234,236,238}U. Angular distributions were extracted for $J^{\pi} = 0^{+} - 8^{+}$ members of the ground-state rotational bands, and were analyzed with use of coupled-channels calculations for scattering from a deformed optical potential. The deformation parameter β_6 is positive for ^{232}Th and ^{234}U, nearly zero for ^{236}U, and negative for ^{238}U. The trends of the deformation parameters and multipole moments are explained qualitatively by a simple model.

PACS numbers: 25.40.Ep, 21.10.Ft, 27.90.+b

The actinide nuclei accessible to scattering experiments are known to be intrinsically deformed and thus their charge and matter (proton and neutron) distributions possess nonzero multipole moments. The moments best studied experimentally and theoretically are the quadrupole and hexadecapole ("2^{λ} pole," where $\lambda = 2$ and 4, respectively). Very little information currently exists on

Proximity to the Rho-Meson Condensation Threshold in Nuclei

H. Toki
National Superconducting Cyclotron Laboratory and Department of Physics, Michigan State University, East Lansing, Michigan 48824

and

J. R. Comfort
Department of Physics and Astronomy, University of Pittsburgh, Pittsburgh, Pennsylvania 15260
(Received 11 May 1981)

Critical conditions for instability in the isovector unnatural-parity channel in nuclei are investigated in terms of the random-phase approximation. The particle-hole residual interaction consists of the π and ρ (2π) meson-exchange attractive components in addition to the short-range repulsive Landau term. It is found that the nonresonant part of the iterated two-pion exchange moves the characteristics of the nuclear phase transition closer to those for rho-meson condensation. This mode may dominate at high density.

PACS numbers: 21.60.-n, 21.60.Jz, 21.65.+f

Although the possible existence of a pion-condensed mode of hadronic matter has been widely discussed,[1,2] careful studies of nucleon-nucleon correlations have led to the conclusion that the critical density is greater than 1.5 times the normal density of nuclear matter.[3-6] Recent discussions have thus focused on the possibility of observing precritical phenomena in ordinary nuclei.[7-9] The proximity of the pion condensation threshold should amplify the pionic field in finite nuclei and thus increase the cross sections of (e,e'),[8] (p,p'),[9,10] and (π,γ) or (γ,π) reactions[11,12] for isovector unnatural-parity transitions at large momentum transfer.

Quantitative discussions of precritical behavior have centered on the 1^+, $T=1$ state of ^{12}C for which the $M1$ form factor $|F_M|^2$ predicted by the Cohen-Kurath wave functions[13] is substantially smaller than the data from (e,e') reactions.[9,14] Analyses in the context of precritical behavior with π- and ρ-meson exchange interactions have led to values of the Landau-Migdal parameter $g' \lesssim 0.4$.[8] However, by inclusion also of the nonresonant part of the two-pion exchange (TPE) in the isovector channel, good agreement with the data was obtained for $g' \sim 0.55$.[14] Analyses of recent (p,p') data for the same transition have shown little evidence of precritical enhancements and are consistent with a value $g' \gtrsim 0.60$.[15,16]

In examining the previous analyses, we realized that the amount of enhancement that could be produced, and the subsequent estimate of g', were very sensitive to the strength of the $\vec{\sigma}\times\vec{q}$ correlations provided by the ρ-meson exchange (RME) and the iterated one-pion exchange (OPE). The TPE strength is commonly related to the $N\bar{N} \to 2\pi$

Excitation of the Giant-Resonance Continuum with Intermediate-Energy Protons

J. M. Moss, T. A. Carey, J. B. McClelland, N. J. DiGiacomo, and S. J. Seestrom-Morris
Los Alamos National Laboratory, Los Alamos, New Mexico 87545

and

G. F. Bertsch and O. Scholten
Institute of Theoretical Physics, University of California, Santa Barbara, Santa Barbara, California 93106, and Cyclotron Laboratory, Michigan State University, East Lansing, Michigan 48824

and

G. S. Adams
Laboratory for Nuclear Science, Massachusetts Institute of Technology, Cambridge, Massachusetts 02139

and

M. Gazzaly and N. Hintz
Physics Department, University of Minnesota, Minneapolis, Minnesota 55455

and

S. Nanda
Physics Department, Rutgers University, New Brunswick, New Jersey 08903
(Received 6 November 1981)

The angular distribution of the continuum in the reaction ^{116}Sn$(p,p')^{116}$Sn at $E_p = 800$ MeV shows a marked decrease in cross section toward small scattering angles ($\theta_L < 6°$). This behavior is well described by a single scattering model which includes the effects of Pauli blocking. Continuum analyzing power data are found to be very close to the values for free p-p and n-p scattering. However, spin-flip probabilities in ^{208}Pb ($E_p = 400$ MeV) and ^{90}Zr ($E_p = 500$ MeV) are significantly smaller than the free nucleon values.

PACS numbers: 24.30.Cz, 24.70.+s, 25.40.Ep, 25.40.Rb

At small momentum transfers ($q < 3$ fm^{-1}) inelastic scattering with energy loss of 5 to 50 MeV leads to the excitation of broad giant resonances (GR) and a nearly featureless continuum, on which the GR's lie. Since, for hadron scattering, the continuum cross section is typically 5 to 10 times that contained in GR's, it is obviously of great interest to try to understand its excitation if only to understand better the characteristics of GR's. The nature of the continuum itself is also of interest, however. From a reaction theory viewpoint, it is important to know what mechanisms are involved in its excitation. Additionally, there may be nuclear structure information obtainable in the continuum.

In this Letter we address both points. We first show that the cross section for the low-excitation-energy continuum excited by 800-MeV protons may be understood in terms of a single-collision model based on Glauber theory.[1] A significant feature of the calculation, which is also seen in the data, is a decrease in the continuum cross section at small angles due to Pauli blocking. Then, looking at continuum analyzing powers and spin-flip probabilities, we present evidence that spin-dependent strength is greatly suppressed in the low-excitation-energy region of the nuclear continuum.

Beams of 400-, 500-, and 800-MeV polarized protons from the Clinton P. Anderson Meson Physics Facility were used to study the excitation energy region from 0 to 50 MeV in ^{90}Zr, ^{116}Sn, and ^{208}Pb. The inelastically scattered protons were momentum analyzed by the high-resolution spectrometer (HRS) and detected in an array of multiwire drift chambers which have been described previously.[2] The spin-flip probability measurements were obtained using the newly developed HRS focal-plane polarimeter.[3] This device consists of a carbon scattering target behind the normal focal-plane chambers plus two additional x-y planes of larger multiwire chambers behind the carbon target. Complete reconstruction of the trajectory is accomplished for all protons scattered in the polarimeter target. The scattering efficiency of the polarimeter is 7.5% at 400 MeV and the average analyzing power is near 0.35.

SHELL-MODEL CALCULATION OF M1 SCATTERING STRENGTHS IN ^{42,44,48}Ca

J.B. McGRORY
Physics Division, Oak Ridge National Laboratory [1], *Oak Ridge, TN 37830, USA*

and

B.H. WILDENTHAL [2]
Cyclotron Laboratory, Michigan State University, East Lansing, MI 48824, USA

Received 11 May 1981

Calculations in the complete $f_{7/2}f_{5/2}p_{3/2}p_{1/2}$ model space are presented for the M1 excitation of the ground states of ^{42,44,48}Ca.

The degree to which excitations of nucleon into "Δ" particles may participate in ostensibly nuclear excitations is a topic of current interest [1–5]. Such participation is suggested as one of several mechanisms [6] responsible for quenching the measured strengths of M1 and Gamow–Teller or (p, n) transitions to values significantly below simple theoretical estimates. Such quenching is experimentally detected to a small degree in the sd shell, to a greater degree in the calcium isotopes (as we shall concentrate upon), and in a succession of heavier nuclei up to the lead isotopes. Earlier evidence for such quenching came principally from magnetic-moment data and a few M1 gamma-decay strengths [7]. Recently, a very significant augmentation of experimental knowledge in this area has resulted from exploitation of high-resolution, back-angle electron scattering [8–10] and of the (p, n) reaction at intermediate energies [11]. A general conclusion of these experiments is that ≈50% of the total ground-state strength of the operator σ or $(\sigma\tau)$ is observed consistent with a significant renormalization of σ.

We deal in this note specifically with recent information on M1 excitation strengths in the Ca isotopes obtained by the Darmstadt group [10]. These experimental results show unambiguously that the total M1 transition strengths in nuclei as light as calcium are significantly quenched relative to simple independent-particle shell-model estimates. Our purpose here is to evaluate the corrections due to configuration mixing to these "extreme single-particle" theoretical estimates which arise from "ordinary" nuclear structure effects (configuration mixing), and to illuminate the relationship between the quenching of magnetic moments and "giant M1 strength". Our goal is to provide a better foundation for judging the degree to which exotic mechanisms may be manifested in the experimental observations.

We choose to analyze the Ca isotopes because (1) of new, high-quality, experimental data available, and (2) it is technically feasible to explore the consequences of making the full transition from the "extreme single-particle" model to a complete $0\hbar\omega$ "mixed-configuration" model for these isotopes. To the extent that excitations of the ^{40}Ca core can be ignored, only neutron excitations are possible for M1 transitions in the Ca isotopes, and the M1 excitations are proportional only to the σ operator, the operator which is suggested to mediate the coupling of the isobar excitation into the nuclear excitation.

The "extreme single-particle" model for the Ca isotopes assumes a closed ^{40}Ca core and wave functions of $N = A - 40$ neutrons, each neutron occupying the $0f_{7/2}$ orbit. The isotope ^{48}Ca thus corresponds

[1] Research sponsered by the Division of Basic Energy Sciences, US Department of Energy under Contract W-7405-eng-26 with the Union Carbide Corporation.
[2] Research sponsored in part by US National Science Foundation, Grant PHY-7822696.

QUENCHING OF MAGNETIC TRANSITIONS AND Δ(1232) DEGREES OF FREEDOM IN NUCLEI: THE ^{48}Ca CASE ☆

A. HÄRTING and W. WEISE
Institute of Theoretical Physics, University of Regensburg, D–8400 Regensburg, West Germany

H. TOKI
Cyclotron Laboratory, Michigan State University, East Lansing, MI 48 824, USA

and

A. RICHTER
Institut für Kernphysik, Technische Hochschule Darmstadt, West Germany

Received 27 May 1981

The quenching of M1 transitions is discussed within the framework of an effective magnetic transition operator renormalized by virtual Δ(1232)–hole excitations. This scheme is applied to the M1 transition from the ground state to the 10.23 MeV (1^+) state in ^{48}Ca, a case which appears to reveal a comparatively simple shell-model structure. It is demonstrated that a large fraction of the observed quenching of the B(M1) value can be related to Δ(1232) degrees of freedom in a way consistent with the quenching of Gamow–Teller transitions.

Recently, the interest in the general role of polarization phenomena involving the Δ(1232) in the renormalization of spin–isospin-dependent transition operators in nuclei [1–5] has increased considerably, mainly because the suggested quenching of these operators in the long-wavelength limit has been observed systematically in magnetic transitions [6] as well as Gamow–Teller (GT) resonances [7]. The common roots of both the magnetic spin- and GT-quenching mechanisms have been emphasized in a number of recent theoretical considerations for finite nuclei [8–12], thereby providing increasing evidence for the way in which Δ(1232) degrees of freedom operate in nuclei even at low energy and momentum transfers.

In the present note we would like to concentrate on the case of the $J^\pi = 1^+$, $T = 4$, state at $E_x = 10.23$ MeV in ^{48}Ca. This state is excited by a strong M1 transition in backward (e, e′) scattering [13]. The ground state of ^{48}Ca has a fairly well closed proton shell [14] and it is also known from neutron pick-up reactions [15] that the average number of $f_{7/2}$ neutrons is very close to the independent particle shell-model expectation, i.e. 8. Ground-state correlations are therefore small. Consequently, the excited 1^+ state has a dominant $(f_{5/2}f_{7/2}^{-1})$ neutron particle–hole structure. This is also corroborated by RPA [16] and very recent shell-model calculations in the complete fp model space [17]. Therefore this state can be expected to provide a particularly useful testing ground for spin–isospin polarization phenomena of non-nucleonic origin.

The independent particle shell model predicts a value $B(\mathrm{M1})\uparrow = 12.0\mu_K^2$ for a pure $f_{7/2} \to f_{5/2}$ transition using the g factor for free neutrons. In contrast, the experimental value is $B(\mathrm{M1}) = (4.0 \pm 0.3)\mu_K^2$, indicating a massive quenching compared to the shell-model value [13]. Our aim here is to demonstrate that a large fraction of the Ml quenching can in fact be attributed to virtual Δ–hole excitations renormalizing the spin g-factor.

A related observation has been made in the

☆ Work supported in part by Deutsche Forschungsgemeinschaft.

0 031–9163/81/0000–0000/S 02.50

BAND CROSSING IN ^{162}Dy: CHARACTERISATION OF NEGATIVE-PARITY YRAST AND YRARE SEQUENCES

P.M. WALKER

Science and Engineering Research Council, Daresbury Laboratory, Warrington WA4 4AD, UK[1] *and Cyclotron Laboratory, Michigan State University, East Lansing, MI 48824, USA*

F.W.N. de BOER

Physics Department, University of Fribourg, c/o SIN, 5234 Villigen, Switzerland[1] *and Nuclear Physics Laboratory, University of Colorado, Boulder, CO 80309, USA*

and

C.A. FIELDS

Nuclear Physics Laboratory, University of Colorado, Boulder, CO 80309, USA

Received 4 June 1981

The crossing of an octupole band by a rotation-aligned two-quasiparticle band has been observed in detail in ^{162}Dy. Both the yrast and yrare states are identified from the band heads ($I = 2$ and $I = 5$) to high spin ($I \sim 14$), with band crossings in both the even-spin and odd-spin sequences.

The form of rotational bands in deformed nuclei illustrates the dynamic competition between collective and intrinsic degrees of freedom. In particular, band crossings make evident the changing circumstances which favour different excitation modes in different angular-momentum domains.

Frequently, the combined influence of the method of population of the states, and the mixing between the crossing bands, results in only the lower (*yrast*) sequence being identified experimentally. One observes yrast anomalies (backbending) but the question of the nature of the unfavoured (*yrare*) states is left open.

The present letter considers one such observation of the negative-parity yrast and yrare states (i.e. the two negative-parity sequences of states that lie lowest in energy) through the band-crossing region. The character of both the bands is deduced from the excitation and deexcitation modes.

This explicit band crossing has been observed in ^{162}Dy, following the ^{160}Gd(α, 2n) reaction at 28 MeV. Using standard γ-ray and conversion-electron techniques (including detailed γ–γ coincidence studies) at least six rotational bands have been identified up to $I \geqslant 10$. The complete results will be published elsewhere [1] but here we concentrate on the two lowest negative-parity bands, illustrated in fig. 1. The negative-parity yrast sequence changes above $I = 7$, from the octupole band to the two-quasiparticle (2qp) band.

The placement of the levels in the two bands as indicated in fig. 1 is based initially on the connecting in-band transitions (and the knowledge of the low-spin members of the octupole band from other work [2]). In the band based on the $I = 5$, 1486 keV level, all even-spin members have both $I \rightarrow I - 2$ and $I \rightarrow I - 1$ branches. These specify uniquely all the band members except the $I = 9$ member; we show later that the $I = 9$, 1940 keV level is strongly mixed with the $I = 9$, 1960 keV level, so that in which band each is placed is somewhat arbitrary. The even-spin levels in the band above the 1148 keV level form a sequence with smooth be-

[1] Present address.

0 031–9163/81/0000–0000/$ 02.50

COMPARISON OF NON-COMPOUND NEUTRON AND PROTON EMISSION IN ^{16}O INDUCED REACTIONS ON ^{238}U AT 310 MeV

J. KASAGI, S. SAINI[1], T.C. AWES, A. GALONSKY, C.K. GELBKE[2], G. POGGI[3] and D.K. SCOTT
Cyclotron Laboratory, Michigan State University, East Lansing, MI 48824, USA

K.L. WOLF
Chemistry Division, Argonne National Laboratory, Argonne, IL 60439, USA

and

R.L. LEGRAIN[4]
Lawrence Berkeley Laboratory, Berkeley, CA 94720, USA

Received 20 May 1981

The emission of energetic neutrons and protons in coincidence with fission fragments was measured for the reactions $^{238}U(^{16}O, nf)$ and $^{238}U(^{16}O, pf)$. Larger cross sections were observed for the emission of high-energy protons than for the emission of high-energy neutrons. The differences in spectral shapes and the implications for the coalescence model are discussed.

In the last few years, it has been established that the collision between complex nuclei at non-relativistic energies may lead to the emission of energetic light particles which cannot be explained in terms of evaporation from completely equilibrated nuclei [1–10]. Assuming that protons and neutrons have similar spectral shapes, it has been shown [11,12] that the energy spectra of deuterons and tritons may be related to the energy spectra of protons by a simple coalescence relation. However, a direct comparison of non-compound proton and neutron cross sections has not yet been performed. In this letter, we present the first such comparison; the reactions used were $^{238}U(^{16}O, pf)$ and $^{238}U(^{16}O, nf)$ at 310 MeV incident energy.

The experiment was performed at the 88 inch cyclotron of the Lawrence Berkeley Laboratory. A UF_4 target of thickness 320 $\mu g/cm^2$, mounted on an 80 $\mu g/cm^2$ carbon backing, was irradiated by $^{16}O^{6+}$ ions of 310 MeV incident energy. The target and fission detector were mounted in a thin-walled scattering chamber [13] fabricated of aluminum. Fission fragments were detected with a surface barrier detector of 60 μm depletion depth and 450 mm^2 active area. This detector was mounted at an angle of $\theta_f = -90°$ with respect to the beam axis and at a distance of 1.5 cm from the center of the target. Four liquid scintillation detectors (NE 213) of diameter and thickness 11.4 cm × 6.0 cm, 12.7 cm × 5.1 cm, 12.7 cm × 7.6 cm and 12.7 cm × 7.6 cm were used to detect neutrons emitted at angles with respect to the beam of 25°, 40°, 55° and 95°, respectively, in coincidence with fission fragments. The flight paths were 2.05 m. In order to reduce the background due to extraneous sources and due to scattering in the experimental vault, these detectors were placed inside shields constructed of lead, concrete and paraffin.

[1] On leave from Bhabha Atomic Research Center, India.
[2] Alfred P. Sloan Fellow.
[3] On leave from University of Florence, Italy.
[4] On leave from CEN, Saclay, France.

SYSTEMATICS OF COLLECTIVE STATES IN LEAD NUCLEI FROM INELASTIC PROTON SCATTERING ☆

J.E. FINCK, G.M. CRAWLEY and J.A. NOLEN Jr.
Cyclotron Laboratory, Michigan State University, East Lansing, MI 48824, USA

and

R. KOUZES
Department of Physics, Princeton University, Princeton, NJ 08544, USA

Received 6 October 1981

From the scattering of 35 MeV protons from ^{206}Pb accurate excitation energies and angular distributions have been determined for the strongly excited collective states. These states are compared to corresponding states in ^{207,208}Pb. A possible explanation of the anomaly in the 5^- strength is given in terms of the core wave functions.

The strongest states excited by direct reactions in the doubly magic nucleus ^{208}Pb are the collective 3^-, 5^-, 2^+, 4^+, 6^+, 8^+ levels between 2.5 and 5.0 MeV of excitation. Many experiments have been performed to examine the corresponding weak-coupling states in ^{207}Pb (c.f. ref. [1] and references contained therein). Several experiments [2–4] have also been performed on ^{206}Pb to observe the analogous collective states in this nucleus. These experiments show a strong correlation in both energy and strength of the collective states in the three nuclei with the exception of the $L = 5$ states. In this letter we report measurements of inelastic proton scattering from ^{206}Pb, and suggest an explanation for the $L = 5$ anomaly in these nuclei.

The experiment was performed using 35 MeV proton beams from the Michigan State and Princeton University cyclotrons. Targets of 0.1 mg/cm^2 enriched to 97.22% were deposited in vacuum on a 20 μg/cm^2 ^{12}C foil. The spectra recorded for this experiment were obtained using either nuclear emulsions in the focal plane of the Michigan State University Enge split-pole magnetic spectrograph, or a position-sensitive proportional counter in the focal plane of the Princeton University QDDD-spectrograph. Both methods of acquiring data offer unique advantages. Data taken with the nuclear emulsions have far better resolution ($\approx$8 keV) and yield accurate excitation energies. Up to an excitation energy of 3.5 MeV, the excitation energies given in figs. 1 and 2 are accurate to ±3 keV. The uncertainties increase by about 1 keV per 500 keV of excitation energy beyond 3.5 MeV due to extrapolation. The proportional counter gives more accurate cross-section data because it is not limited by the number of counts in a peak. Because of the finite length of the counter, and the large dispersion of the QDDD, the measurements were made in three passes to cover the energy range from the ground state up to an excitation energy of approximately 5.5 MeV.

Angular distributions of the even-parity collective states are shown in fig. 1. The data are compared to the empirical angular distributions for the analogous states in ^{208}Pb [5] and to collective model calculations using the program DWUCK [6]. The agreement between the calculated angular distributions and the

☆ This material is based upon work supported by the National Science Foundation under Grant No. Phy 80-17605 and Phy 81-05673.

A PSEUDO-SPIN SYMMETRY IN THE IBFA MODEL

O. SCHOLTEN

National Superconducting Cyclotron Laboratory, Michigan State University, East Lansing, MI 48824, USA [1]
and Institute for Theoretical Physics, University of California, Santa Barbara, CA 93106, USA

Received 1 October 1981

It is shown that the level doubling, observed in certain collective medium heavy odd-mass nuclei can be explained in terms of a pseudo-spin symmetry in the IBFA model. The selection rules for single particle transfer agree with experiment.

In the IBA model [1] the low-lying collective states in a medium mass even–even nucleus are described in terms of a system of s- and d-bosons. In the IBFA model [2–4] the low-lying states in medium heavy odd-mass nuclei are described by coupling the degrees of freedom of a single fermion to the s–d boson system. An exact pseudo-spin symmetry occurs in the IBFA hamiltonian [3] whenever the odd fermion can occupy two single particle (SP) orbits which differ in spin by one unit, have equal SP energies and have equal occupation probabilities. In this case the energy levels occur in doublets, differing in spin by one unit.

Since the present symmetry is related to pseudo-spin it will prove easier to work in an L–S coupling scheme rather than the usual j–j coupling basis. The relation between the two is given by

$$|\alpha,(R,l)L,1/2;J\rangle = \sum_{j=l-1/2}^{l+1/2}(-1)^{R+l+J+1/2}\sqrt{(2L+1)(2j+1)} \times \begin{Bmatrix} R & l & L \\ 1/2 & J & j \end{Bmatrix} |\alpha,R,(l,1/2)j;J\rangle, \quad (1)$$

where R is the boson total angular momentum and α denotes the other quantum numbers necessary to label the boson state uniquely. The l introduced in eq. (1) is not necessarily the real SP orbital angular momentum, but is chosen such that the j-values of the two involved SP orbits can be obtained from it by coupling a pseudo-spin, i.e. $l=(j+j')/2$. The symmetry is based on the fact that in the IBFA model the boson fermion interaction stems from a nucleon-nucleon quadrupole force which acts only on the pseudo-orbital angular momentum. Because of the spin independence of the interaction, the energies depend only on $(\alpha,(R,l)L)$ and the levels in the spectrum thus occur in doublets with spins $l=L\pm 1/2$.

The spin independence of the boson–fermion interaction can be demonstrated explicitly. We will outline here only the proof for the quadrupole term, which can be written as [4]

$$V_Q = \gamma\sum_{jj'}(-1)^{j'-1/2}\sqrt{(2j+1)(2j'+1)}\sqrt{5}/4\pi \times \begin{pmatrix} j & 2 & j' \\ -1/2 & 0 & 1/2 \end{pmatrix} Q_B^{(2)}\cdot(a_j^\dagger \tilde{a}_{j'})^{(2)} \quad (2)$$

where $Q_B^{(2)}$ is the boson quadrupole operator and $a_j^\dagger$ (a_j) the fermion creation (annihilation) operator while $\tilde{a}_{j,m}=(-1)^{j-m}a_{j,-m}$. With the use of some angular momentum algebra it can be shown that

$$\langle\alpha,(R,l)L,1/2;JM|V_Q|\alpha',(R',l)L',1/2;JM\rangle = \gamma\delta_{L,L'}\frac{5(2l+1)}{\sqrt{4\pi}}(-1)^{R'+L} \times \begin{Bmatrix} R' & R & 2 \\ l & l & L \end{Bmatrix}\begin{pmatrix} l & l & 2 \\ 0 & 0 & 0 \end{pmatrix}\langle\alpha,R\|Q_B^{(2)}\|\alpha',R'\rangle, \quad (3)$$

[1] Permanent address.

IN-PLANE CORRELATIONS BETWEEN PROTONS AND DEUTERONS FOR ^{16}O-INDUCED REACTIONS ON ^{27}Al AND ^{197}Au AT 310 MeV

W.G. LYNCH, L.W. RICHARDSON, M.B. TSANG, R.E. ELLIS and C.K. GELBKE
National Superconducting Cyclotron Laboratory, Michigan State University, East Lansing, MI 48824, USA

and

R.E. WARNER
Oberlin College, Oberlin, OH 44074, USA
and National Superconducting Cyclotron Laboratory, Michigan State University, East Lansing, MI 48824, USA

Received 19 August 1981

In-plane correlations between two light particles have been investigated for ^{16}O induced reactions on ^{27}Al and ^{197}Au targets at 310 MeV incident energy. Within the statistical accuracy of the experiment no differences could be established for the shapes of singles and coincidence proton spectra. The importance of kinematical correlations imposed by energy and momentum conservation for finite equilibrated systems is pointed out. The observed angular correlations are not explained by simply assuming a maxwellian spectrum in the rest frame of a single moving source.

The attainment of local thermal equilibrium in heavy ion induced reactions is an important assumption underlying many theoretical models [1–7]. A large set of single particle inclusive data can be described by this assumption [2,5,8–12] which implies that the emission of light particles should be dynamically uncorrelated. Until now, light particle correlations testing the thermalization assumption have been measured only at relativistic energies (E/A = 400 and 800 MeV) where the existence of a non-thermal knockout component was demonstrated [13,14]. In this letter we report the first such measurement at nonrelativistic energies.

Aluminum and gold targets of 16 and 10 mg/cm^2 thickness were bombarded with 310 MeV $^{16}O^{6+}$ ions from the 88 inch cyclotron of the Lawrence Berkeley Laboratory. Single and coincident protons and deuterons were detected with four $\Delta E - E$ telescopes consisting of solid state silicon–ΔE and NaI(Tl)–E detectors. The telescopes were mounted in a plane at the angles of −110°, −30°, +30° and +75° with respect to the beam axis, subtending solid angles of 62, 49, 49 and 62 msr, respectively. Coincidence and downscaled singles events were recorded on magnetic tape and analyzed off-line.

The singles and coincidence proton spectra measured in this experiment are shown in fig. 1 by the solid points and the histograms, respectively. The singles spectra were found to be consistent with recent measurements of the same systems [12]. Within the statistical accuracy of the present experiment the shapes of singles and coincidence spectra are found to be very similar, indicating that the assumption of statistical emission is not strongly violated.

In order to be more sensitive to the existence of two-particle correlations we present our results in terms of the correlation function $\sigma_{12}/(\sigma_1\sigma_2)$ where

$$\sigma_{12} = \sigma_0 \int_{\Delta E_1} \mathrm{d}E_1 \int_{\Delta E_2} \mathrm{d}E_2 \; \frac{\mathrm{d}^4\sigma(\theta_1, E_1, \theta_2, E_2)}{\mathrm{d}E_1 \mathrm{d}E_2 \mathrm{d}\Omega_1 \mathrm{d}\Omega_2} \tag{1}$$

and

$$\sigma_k = \int_{\Delta E_k} \mathrm{d}E_k \; \frac{\mathrm{d}^2\sigma(\theta_k, E_k)}{\mathrm{d}E_k \mathrm{d}\Omega_k}, \quad k = 1, 2. \tag{2}$$

The constant σ_0 was arbitrarily fixed by requiring $\sigma_{12}/(\sigma_1\sigma_2) = 1$ for the proton–proton correlation corresponding to the variables $\theta_1 = -30°$, $\theta_2 = +30°$, ΔE_1

PAIRING MODEL PREDICTIONS FOR (p, t) EXPERIMENTS ON THE CADMIUM ISOTOPES ☆

G.M. CRAWLEY, W. BENENSON, G. BERTSCH, S. GALES [1], D. WEBER [2] and B. ZWIEGLINSKI [3]
Cyclotron Laboratory, Michigan State University, East Lansing, MI 48824, USA

Received 1 December 1981

The even–even cadmium isotopes have been studied by the (p, t) reaction at 42 MeV. A broad resonance-like structure is observed between 6 and 7 MeV excitation energy which has similar properties to the feature observed in (p, t) reactions in the tin isotopes. A second smaller bump at higher excitation energy appears to arise from pickup of two particles from deep orbits.

The distribution of one-hole strength in a large number of nuclei has been studied both experimentally (see ref. [1] and references therein) and theoretically [2,3]. Recently, a broad resonance has been observed near 8 MeV excitation energy in two particle pickup reactions on the tin isotopes [4,5]. These structures appear to arise from pickup of one neutron from a deep lying orbit ($g_{9/2}$) and one from a valence orbit [6,7].

In order to gain further insight into these broad structures the (p, t) reaction was carried out on the even–even isotopes of cadmium, viz ^{106}Cd, ^{110}Cd, ^{112}Cd, ^{114}Cd, ^{116}Cd using the 42 MeV proton beam from the MSU K50 cyclotron. The tritons were detected on the focal plane of the Enge split pole spectrograph using a position sensitive proportional counter backed by a plastic scintillator. Triton spectra measured at a laboratory angle of 20° are shown in fig. 1. Broad structure is observed in all the cadmium isotopes as in the tin case, but there appears to be a somewhat more varied and fragmented structure in the cadmium spectra particularly for the higher isotopes.

☆ Supported by the US National Science Foundation under grant PHY 80-17605.

[1] Permanent address: Institut de Physique Nucleaire, Orsay, France.

[2] Present address: Aerospace Corp., Los Angeles, CA, USA.

[3] Permanent address: Institute of Nuclear Research, Warsaw, Poland.

Another important feature observed in the cadmium spectra is the appearance of a second broad bump at an even higher excitation energy. This second peak is marked with an arrow in the spectra in fig. 1.

In the ^{104}Cd spectra it is possible to resolve individual levels which have been previously reported [8]. Using the ^{62}Ni (p, t) ^{60}Ni reaction and ^{108}Cd (p, t) ^{106}Cd reactions (from the ^{108}Cd impurity on the ^{106}Cd target) as calibrations, the Q-value for the ^{106}Cd (p, t) ^{104}Cd reaction was measured as −10.802 ±0.015 MeV. The ground state of ^{104}Cd was bracketed by the ^{60}Ni ground state and first excited states. The resulting mass excess is 83.990 ±0.021 MeV. This number disagrees significantly with the mass excess of ^{104}Cd recently measured [9] as 83.720 ±0.030 MeV using the β^+ decay of ^{104}Cd. This most recent measurement also disagrees with an earlier measurement [10] of the decay value by 164 keV even though the error on the earlier measurement was given as ±50 keV. In addition, in as much as the final mass excess obtained in the β^+ decay experiment depends on a much earlier measurement [11] of the decay of ^{104}Ag to an excited state of ^{104}Pd, the final value is obtained by a somewhat indirect route. Nevertheless, an independent measure of the mass excess of ^{104}Cd to resolve the discrepancy between the (p, t) and the β^+ measurement would appear to be useful.

The excitation energies of the enhancement in the cadmium spectra are plotted against the neutron number, N, of the target in fig. 2 together with the

PHYSICAL REVIEW C VOLUME 23, NUMBER 3 MARCH 1981

Mass of ^{6}Li and the excitation energy of its 3.56-MeV state

R. G. H. Robertson and J. A. Nolen, Jr.
Cyclotron Laboratory and Physics Department, Michigan State University, East Lansing, Michigan 48824

T. Chapuran* and R. Vodhanel
Physics Department, University of Illinois, Champaign, Illinois 61820
(Received 30 October 1980)

The excitation energy of the second excited state of ^{6}Li has been measured to be 3562.88 ± 0.10 keV by comparing the energy of resonance fluorescence radiation from this state to calibration lines from a ^{56}Co source. Also the Q value of the ^{6}Li$(p,\alpha)^3$He reaction has been determined relative to the ^{19}F$(p,\alpha)^{16}$O reaction, giving a result for the ground state mass excess of ^{6}Li of 14 085.5 ± 1.1 keV, somewhat below the tabulated value of 14 087.3 ± 0.8 keV. These measurements improve the sensitivity of experiments searching for isovector parity violation in ^{6}Li.

[NUCLEAR REACTIONS ^{6}Li$(\gamma,\gamma)^6$Li, bremsstrahlung source, E_x = 3.56 MeV, measured E_x. Ge(Li) detector. ^{6}Li$(p,\alpha)^3$He, E_p = 10.5 MeV, measured Q. Magnetic spectrograph.]

I. INTRODUCTION

The 0$^+$, T = 1 state of ^{6}Li at 3.56 MeV is energetically able to decay into a deuteron and an alpha particle but is forbidden to do so by conservation of parity and of isospin. A measurement of the decay probability therefore gives a measure specifically of the ΔT = 1 part of the parity-nonconserving interaction. The ^{6}Li case has acquired new significance with the emergence of unified gauge theories of the weak and electromagnetic interactions, which imply the existence of a hadronic weak neutral current. Isovector parity violation is suppressed in conventional descriptions of charged current interactions but is not necessarily suppressed if a hadronic weak neutral current exists.[1]

This decay is now being studied by a group at the Université de Montréal[2], and by a Michigan State University–Argonne National Laboratory–Chalk River Nuclear Laboratory collaboration.[3] In these experiments and several previous ones,[4] the excitation function of the inverse reaction ^{4}He$(d,\gamma)^6$Li or ^{2}H$(\alpha,\gamma)^6$Li is investigated in the region of the 0$^+$, T = 1 state. The presence of parity violation would be indicated by a weak resonance superimposed on the direct capture continuum. A limit to the experimental sensitivity is imposed by the range of energies which must be searched over in order to be certain that the resonance is included. The major contribution to this uncertainty originates in the mass difference between the 0$^+$, T = 1 state of ^{6}Li and ^{4}He + ^{2}H. A direct measurement of this difference to the desired accuracy does not appear to be practical, and in this paper we describe independent measurements of the excitation energy and of the ground state mass of ^{6}Li.

It may be useful at the outset to consider what precision is needed in this program of measurements. A lower limit to the search range in the parity-violation experiment is set by the energy spread and instability of the incident beam. Measurements at Chalk River[3] have demonstrated that, at 6.24 MeV, the energy appropriate for ^{2}H$(\alpha,\gamma)^6$Li via the 3.56-MeV state, a resolution close to 2 keV can be reliably achieved, with an instability less than 1 keV. (The natural and Doppler widths are smaller.) It can be shown that the optimum search range is approximately three times the resolution, or about 6 keV. If one wishes 95% confidence that the resonance lies within the range, then the combined standard deviation in beam energy and masses must be 1.5 keV or less. A beam energy determination to 1 keV is feasible, implying a similar accuracy requirement in the resonance energy. Because of the laboratory-to-center-of-mass kinematic conversion, the precision required in the mass excesses is about 0.3 keV. Neither the ground state mass of ^{6}Li nor the excitation energy of the 3.56-MeV state is known to this accuracy. Two recent measurements[5,6] establish the excitation energy to about 0.5 keV, but there is a serious discrepancy (almost 6 keV) between these results and another of lower precision.[7]

The ground state mass of ^{6}Li has not been determined by direct mass spectroscopic techniques, and its present value (with a quoted uncertainty of

PHYSICAL REVIEW C VOLUME 23, NUMBER 4 APRIL 1981

Spin of deep hole states from $(\vec{p},d)$ reactions

G. M. Crawley and J. Kasagi
Cyclotron Laboratory, Michigan State University, East Lansing, Michigan 48824

S. Gales and E. Gerlic
IPN, B.P. N° 1-91406, Orsay, France

D. Friesel and A. Bacher
IUCF, Indiana University, Bloomington, Indiana 47405

(Received 22 October 1980)

Analyzing power measurements from the $(\vec{p},d)$ reaction on ^{90}Zr and ^{120}Sn have been made using a 90 MeV polarized proton beam. The spin of the broad structure near 5 MeV excitation energy in ^{119}Sn has been unambiguously determined to be 9/2 from comparison with the empirical analyzing power for the ground state of ^{89}Zr and from distorted wave Born approximation calculations.

[NUCLEAR REACTIONS ^{90}Zr$(\vec{p},d)$, ^{120}Sn$(\vec{p},d)$ $E=90$ MeV; polarized beam, measured $\sigma(\theta)$, $A_y(\theta)$ DWBA analysis, deduced by J^π, resolution 100 keV.]

In a large number of previous studies of deep-hole states in medium and heavy nuclei, the transferred orbital angular momentum l has been determined from the measurement of the angular distribution. However, the angular distribution is not sensitive to the total angular momentum j of the final state and this assignment has therefore generally been made only on the basis of the theoretical expectation of the position of a particular shell model orbit. Since the predictions of the single particle strength function have been made for definite values of total angular momentum, it is important to determine the j unambiguously.

Distorted wave Born approximation (DWBA) calculations indicate that a strong j dependence is expected for the analyzing power (A_y) of the $(\vec{p},d)$ reaction at incident energies around 100 MeV. At present there is rather little experimental information on this problem. Some A_y measurements for $(\vec{p},d)$ reactions on a few light nuclei at $E_p=65$ MeV have been reported[1] and some unpublished measurements from a few 0s1d shell nuclei are available.[2] Measurements at even higher energies from 200 to 400 MeV on ^{13}C also indicate a strong j dependence of the analyzing power.[3] Because of these indications of j dependence and because earlier measurements of the (p,d) reaction at 90 MeV on a series of Sn isotopes showed that deep hole states near 5 and 8 MeV excitation energy were strongly excited,[4] differential cross sections and analyzing powers were measured for $(\vec{p},d)$ reactions on ^{90}Zr and ^{120}Sn using a 90 MeV polarized beam from the Indiana University Cyclotron.

The beam polarization was measured before and after each run using a polarimeter placed in the beam line after the first cyclotron and before injection into the second cyclotron. Earlier measurements had established that there was no loss of beam polarization during the final acceleration stage. The measured polarization in both spin-up and spin-down modes was about 70% and proved to be extremely stable. The spin direction was flipped automatically every minute during the data taking runs to reduce systematic errors. A further check was made by operating two detectors, one on each side of the beam, and equivalent measurements made at the same laboratory scattering angle were in good agreement.

The outgoing particles were detected in a solid state detector telescope consisting of a Si(Li) ΔE detector, an intrinsic Ge(E) detector, and a final veto detector also of germanium. To improve the speed of data collection, particle identification was carried out using Elsint identifier boxes which gave excellent separation between deuterons and tritons. The energy resolution was about 100 keV full width at half maximum. The spectra were calibrated using the (p,d) reactions on ^{58}Ni and Mylar targets.

Deuteron spectra from the ^{90}Zr$(\vec{p},d)^{89}$Zr and ^{120}Sn$(\vec{p},d)$ ^{119}Sn reactions, taken with proton spin up and down, are shown in Fig. 1. These spectra show the strong excitation of the deep hole states in ^{119}Sn near 5.5 MeV and in ^{89}Zr near 4.5 MeV as well as the isobaric analog states (IAS) particularly in ^{89}Zr at an excitation energy near 10 MeV. An inspection of these spectra also shows immediately that the analyzing power is a rather clear indi-

Precompound emission of light particles in the reaction $^{16}O + ^{238}U$ at 20 MeV/nucleon

T. C. Awes, G. Poggi,* and C. K. Gelbke
Cyclotron Laboratory, Michigan State University, East Lansing, Michigan 48824

B. B. Back and B. G. Glagola
Chemistry Division, Argonne National Laboratory, Argonne, Illinois 60439

H. Breuer and V. E. Viola, Jr.†
Departments of Physics and Chemistry, University of Maryland, College Park, Maryland 20742
(Received 8 December 1980)

Double differential cross sections have been measured for energetic p, d, t, and α particles emitted in reactions of 315 MeV ^{16}O ions on ^{238}U. In coincidence with light-particle emission, the momentum transfer to the target is determined by measuring the folding angle between the two fission fragments resulting from the sequential decay of the target nucleus. It is concluded that the emission of these particles occurs predominantly in fusionlike "central" collisions and at an early stage of the reaction. The energy and angular distributions are described by thermal emission from a source moving with approximately half of the beam velocity. Alternatively, the energy spectra can be explained by emission from a rotating hot spot. The cross sections for d, t, and α emission can be described in terms of a generalized form of the coalescence model which takes into account the Coulomb repulsion from the target nucleus.

[NUCLEAR REACTIONS $^{238}U(^{16}O, Xf)$, $x = p$, d, t, α, $E = 315$ MeV; measured $\sigma(E_x, \theta_x)$ and fission fragment folding angle distribution. Analysis in terms of hot spot, moving source, and coalescence models.]

I. INTRODUCTION

The emission of light particles in heavy-ion-induced reactions contains important information about the reaction mechanism. At low energies ($E/A \lesssim 5$ MeV above the Coulomb barrier) there is clear experimental evidence[1-4] that the majority of light particles are due to thermal emission from the compound nucleus or from fully accelerated and equilibrated fragments. On the other hand, nonequilibrium emission of light particles has been observed[5-24] for reactions induced by lighter projectiles ($A \approx 16$) and at higher energies ($E/A \gtrsim 8$ MeV). Originally, the energetic light particles that were observed in these experiments were associated with projectile breakup reactions.[5] However, subsequent coincidence experiments have demonstrated[10,12,15-20,22] that reactions where the major part of the projectile is absorbed by the target nucleus make an important contribution to the emission of light particles. These reactions have been variously termed as "incomplete fusion"[18] or "massive transfer"[15,16] reactions or "central"[17] collisions.

Several possible mechanisms have been proposed to explain the emission of noncompound energetic light particles. In qualitative terms, it has been suggested[15-18] that energetic light particles are emitted in a transfer or projectile breakup process where the larger fraction of the projectile mass is absorbed by the target nucleus. On a more quantitative basis, the possible formation of a "hot spot," i.e., a locally heated region of the nucleus, has been suggested.[8,14,25-27] Such a hot spot could attain much higher temperatures than the compound nucleus. Immediately after its formation, the hot spot would cool by thermal diffusion into the adjacent cold nuclear matter or by the emission of energetic light particles. The predicted energy spectra exhibit exponential slopes that correspond to significantly higher temperatures than the compound nucleus temperature. Rather good agreement with experimental data has been obtained in several examples.[26] In addition to an interpretation in terms of the hot spot model, several features of the single-particle inclusive cross sections could be explained[6,23] in terms of preequilibrium[28-30] and intranuclear cascade[31] calculations. Furthermore, the prompt emission of light particles[32,33] (PEP's), and the enhanced alpha-particle emission[34] from superdeformed nuclei have been proposed as additional reaction mechanisms that could produce energetic light particles in the exit channel.

Up to now, most of the experimental effort has been devoted to coincidence studies which were designed to elucidate certain aspects of the emission of precompound light particles. These experiments are generally very phase space selective and the resulting cross sections are difficult

Systematics of the $\sigma\tau_-$ strength in nuclei

G. Bertsch, D. Cha, and H. Toki
National Superconducting Cyclotron Laboratory and Department of Physics, Michigan State University, East Lansing, Michigan 48824
(Received 10 February 1981)

The structure of the $\sigma\tau_-$ strength function is studied with a zero range interaction. The systematics of the giant Gamow-Teller state requires an interaction strength for $V_{\sigma\tau}$ of about 200–240 MeV fm^3. While most of the strength goes to a state at high excitation, we find that ~20–30% of the strength remains at low excitation energy. The $L = 1$ states show considerable J splitting, with a major peak at ≈20 MeV excitation. This peak contains components of $J = 0$, 1, and 2. Comparison with the experimental $L = 1$ energy shows that the momentum dependence of the $\sigma\tau$ interaction is small.

[NUCLEAR STRUCTURE. Gamow-Teller states and $L = 1$ states in adjacent odd-odd mass nuclei of double closed shells. TDA and RPA calculation with zero range interaction.]

INTRODUCTION

The (p,n) reaction studies at intermediate energies have brought a tremendous advance in our empirical knowledge of the distribution of spin excitation strength in nuclei.[1–4] Qualitatively, the strength function has a peak in a state located at or above the position of the analog state. This state, the giant Gamow-Teller resonance, had been anticipated by theory for many years.[5] In this article we wish to correlate the new data with a simple theoretical model. Our purpose is to extract from the data the properties of the residual interaction, rather than simply compare data with a particular interaction model, as has been done in other calculations of the Gamow-Teller strength.[6] Our model is the Tamm-Dancoff approximation (TDA) based on the shell model wave functions from either a Woods-Saxon potential or a Skyrme Hartree-Fock calculation. We shall use a simple δ-function interaction and adjust the interaction strength so as to reproduce the main peak of the $\sigma\tau_-$ strength function. The model then gives predictions for the distribution of strength among 1p-1h configurations. As will be seen, roughly 20% of the strength appears in a state at much lower energy than the giant Gamow-Teller peak.

The same phenomenological interaction may also be applied to higher multipoles, for example, excitations induced by operators of the form $[Y_L(\theta)\sigma]_J\tau_-$. In principle, these higher multipoles will be sensitive to parts of the interaction that are omitted in the δ-function treatment of the 1^+ excitations. Specifically, the momentum dependence of the interaction might affect the energies of the state with $L > 0$. However, we expect these effects to be small, and much can be learned with the momentum independent interaction. We shall discuss the effect of the momentum dependent interaction (finite range force) at the end. In examining the $L = 1$ strength function, we find a substantial splitting between different J states.

CALCULATIONAL DETAILS

Our model Hamiltonian consists of the single-particle Hamiltonian and the residual interaction. The single-particle Hamiltonian is spin dependent and possibly momentum dependent. As a model, we use a Woods-Saxon potential of standard parameters: $V_0 = 50$ MeV, $r_0 = 1.27$ fm, $A = 0.67$ fm. We shall also calculate the single-particle Hamiltonian within the Hartree-Fock theory with the Skyrme III interaction for comparison purposes.[7] This model has an effective mass $m^*/m = 0.76$, close to what is expected from more fundamental Brueckner-Hartree-Fock theory. Besides the effective mass, another important question is the magnitude of the spin-orbit potential, since much of the excitation energy of the Gamow-Teller state arises from the spin-orbit splitting. The spin-orbit splitting of particles traveling at the Fermi momentum is about 6 MeV, but the direct observation of the splitting is difficult. The most direct evidence on the

Search for enhancements due to pion condensation precursors in (p,p') reactions on ^{12}C

J.-L. Escudié, S. M. Austin,* A. Boudard, G. Bruge, A. Chaumeaux, L. Farvacque, D. Legrand, J. C. Lugol, and B. Mayer
Centre d'Etudes Nucléaires Saclay, BP 2, F-91190 Gif-sur-Yvette Cédex, France

P. Belery, P. T. Debevec,† T. Delbar, J. Deutsch, G. Grégoire, and R. Prieels
Université Catholique de Louvain, B-1348 Louvain-la-Neuve, Belgium

J. M. Cameron
University of Alberta, Edmonton, Alberta T6G 2N5, Canada

C. Glashausser
Rutgers University, New Brunswick, New Jersey 08903

C. A. Whitten
University of California at Los Angeles, Los Angeles, California 90024

(Received 13 April 1981)

Cross sections for the $^{12}C(p,p')$ reaction leading to the 1^+ states at 15.1 MeV ($T=1$) and 12.7 MeV ($T=0$) were measured at a bombarding energy of 402 MeV. These data, covering a range of momentum transfer q from 0.45 to 2.65 fm^{-1} ($0.6-3.7m_\pi$) provide a test of the effects, precursor to a pion condensate, predicted to be important for the $T=1$ state near $q=2-3m_\pi$. The cross sections for the two 1^+ states are very similar for large q, perhaps indicating that the precursor effects are small.

[NUCLEAR REACTIONS $^{12}C(p,p')$; measured $\sigma(\theta)$, $q_c \simeq (2-3)m_\pi$ 15.1 MeV $1^+T=1$ and 12.7 MeV $1^+T=0$ levels; $E_p=402$ MeV; precursor effects discussed.]

Migdal[1] and independently Sawyer[2] first called attention to a possible new phase of sufficiently large hadronic systems in which pions would have condensed from the vacuum. Subsequent theoretical work[3] showed that due mainly to repulsive nucleon-nucleon correlations the onset of this new phase could be expected only for systems with about twice the normal nuclear density; such densities presumably occur in dense astronomical objects and are possibly reached in heavy ion collisions.[4] Indirect indications for the existence of this "pion-condensed" phase in neutron stars are still controversial,[5] and given our present state of knowledge, evidence for the condensed phase obtained from heavy ion collisions is likely to be ambiguous. Fortunately, the condensation mechanism also implies,[6,7] even at normal densities, that there are so-called "precursor" effects: enhancements of the cross sections for nuclear transitions which carry the quantum numbers of the pion ($\Delta S=\Delta T=1$). These enhancements should be largest at momentum transfers of $2-3m_\pi$ ($m_\pi=140$ MeV/$c=0.7$ fm^{-1}).[8-13] Observation of such effects should also yield information on the effective short-range repulsive nucleon-nucleon interaction (value of the Migdal parameter g') which must be known to predict when pion condensation will occur.

Recent investigations of cross sections for magnetic electron scattering in ^{12}C (Refs. 10–12) and ^{13}C (Ref. 13) seem to indicate that the precursor effects are surprisingly large, corresponding to values of $g'=0.4-0.5$, compared to the values greater than 0.6 found from the low momentum properties of nuclear states. In view of these results it is then crucial to check the conclusions with a probe, such as inelastic proton scattering,[6,9,11,12] which couples more directly to the pion field than (e,e').[14]

The choice of bombarding energy is crucial in such experiments if we wish to relate the experimental results and theoretical predictions with confidence. For the validity of current reaction models, energies above 200 MeV seem necessary.[15-17] For example, the calculations of Comfort and Love[15] at $E_p=122$ MeV apparently indicate that precursor effects must be small in (p,p') transitions leading to the 1^+, $T=1$ state at 15.1 MeV in ^{12}C. Unfortunately, their calculations, while nicely reproducing the data for this state at low q, fail for the nearby 1^+, $T=0$ state at 12.7 MeV. As a result, one cannot have confidence

PHYSICAL REVIEW C VOLUME 24, NUMBER 3 SEPTEMBER 1981

Giant $M1$ states in Zr isotopes within the simple shell model

H. Toki, D. Cha, and G. Bertsch
National Superconducting Cyclotron Laboratory and Department of Physics, Michigan State University, East Lansing, Michigan 48824
(Received 16 April 1981)

The newly observed $M1$ states in the (p,p') experiment on the Zr isotopes are considered within the simple shell model. The calculation with a constant strength δ function interaction reproduces the excitation energies and the slight increase of the $M1$ strength at small momentum transfer with mass number. We need about a factor of 2 quenching to reproduce the cross sections at small angles, which is in accordance with the general finding for magnetic transitions.

[NUCLEAR STRUCTURE $^{90-96}$Zr; shell model calculations, 1^+ states.]

Very recently Anantaraman *et al.* have performed a (p,p') experiment at $E_p = 200$ MeV on the Zr isotopes and found for the first time giant $M1$ states in these nuclei.[1] This is a very interesting result because before this experiment no $M1$ states had been reported in heavy nuclei ($A \gtrsim 90$) in both hadron and electron experiments.[2] If we look at shell structures of these heavy nuclei, we expect that the $l \cdot s$ particle-hole pairs, $g_{7/2}$-$g_{9/2}^{-1}$, $h_{9/2}$-$h_{11/2}^{-1}$, $i_{11/2}$-$i_{13/2}^{-1}$, . . . , should produce $M1$ states a few MeV above the $l \cdot s$ splitting energy. The fact that $M1$ strengths were not observed in heavy nuclei has been a puzzle for a long time. Thus, the recent (p,p') experiment[1] provides new valuable information for the discussion of $M1$ strength in nuclei. In this paper we compare the experimental data with a simple shell model calculation based on the general consideration of the single-particle wave functions and the residual interaction.

There has been some controversy recently about the appropriate single-particle model, engendered by the failure to find the $M1$ strength in ^{208}Pb.[2] Brown *et al.*[3] have argued that the single-particle energy differences obtained from an empirical analysis should be multiplied by a factor $m/m^* \sim 1/0.7$ to use in calculations of the $M1$ strength. We disagree with this prescription on two grounds. First, changes in effective mass for collective states can only arise from collective energy shifts, and cannot be applied to the $M1$ state, which has only shifted by a couple of MeV. Second, the effective mass m^* applies to the single-particle kinetic energy, and not to energy differences originated from the spin-orbit field. All of the single-particle energy in the $M1$ state is due to the spin-orbit field. In our calculation, we take single-particle wave functions from Woods-Saxon well calculations. These wave functions are identical to Hartree-Fock wave functions for practical purposes. The crucial spin-orbit interactions we adopt from the phenomenological optical model analysis of Becchetti and Greenless.[4] This results in 6 MeV spin-orbit splitting between the $g_{7/2}$ and $g_{9/2}$ orbits for ^{90}Zr.

The residual interaction can be taken to be zero range for describing excitation of long wavelength states. The noncentral interactions for shell model matrix elements, and the finite range aspects of the force can be included by a small shift in the strength parameter of the zero-range force.[5]

$$V_{\rm res} = \bar{V}_\sigma \delta(\vec{r}_1 - \vec{r}_2)\, \vec{\sigma}_1 \cdot \vec{\sigma}_2 \ , \qquad (1)$$

where $\bar{V}_\sigma = V_\sigma + V_{\sigma\tau}$ with V_σ being the strength of the non-τ-dependent interaction and with $V_{\sigma\tau}$ being that of the τ-dependent interaction. We note that the strength $V_{\sigma\tau}$ deduced from the giant Gamow-Teller state in medium and heavy nuclei is 220 MeV fm^3.[5] The known $M1$ state in ^{48}Ca can additionally be used to determine V_σ and we find that $V_\sigma \cong V_{\sigma\tau}$. Microscopic calculations based on the Brueckner theory with the Reid potential also indicate that $V_\sigma \cong V_{\sigma\tau}$.

Using the above model Hamiltonian, we calculated the excitation energies and the (p,p') cross sections at 0°. In order to obtain the cross sections, we used the empirically obtained distortion factor N_D and the $\sigma\tau$ interaction strength $J_{\sigma\tau}$ from the work by Goodman *et al.*[6] Furthermore, the small isospin independent spin-spin term is added to the $\sigma\tau$ interaction strength for the neutron particle hole excitation by the scattering proton. The isospin independent strength J_σ is estimated from the work by Love and Franey[7] to be

$$(J_\sigma + J_{\sigma\tau})/J_{\sigma\tau} \simeq 1.15 \qquad (2)$$

A further assumption is that the distortion factor does not change greatly from $E_p = 120$ to 200 MeV. Although we believe this to be qualitatively correct, it needs to be checked quantitatively. The calculated results along with the experimental data are depicted in Table I. The almost constant excitation energies

Nuclear structure of even-A chromium isotopes in the band-mixed projected Hartree-Fock model

Surender Saini*
National Superconducting Cyclotron Laboratory, Michigan State University, East Lansing, Michigan 48824 and Nuclear Physics Division, Bhabha Atomic Research Center, Bombay 400085, India

M. R. Gunye
Theoretical Reactor Physics Section, Bhabha Atomic Research Center, Bombay 400085, India
(Received 13 April 1981)

Nuclear structure calculations for the states in even-A isotopes $^{48-54}$Cr are performed in the framework of the projected Hartree-Fock model by employing a realistic nucleon-nucleon interaction. An inert ^{40}Ca core is assumed and all the valence nucleons are treated explicitly in the configuration space of the full fp shell. The energy levels, static electromagnetic moments, and transition probabilities are evaluated from the band mixing calculations wherein a large number of energetically close intrinsic states of the nuclei are taken into account. These calculations yield a $K^\pi=2^+$ and $K^\pi=4^+$ highly deformed band for ^{50}Cr and ^{52}Cr, respectively, when a neutron from the predominantly $(f_{7/2})^n$ lowest prolate intrinsic configuration is promoted to the higher unoccupied (fp) orbits. The results of the present calculations are in fairly good agreement with the available experimental data.

[NUCLEAR STRUCTURE Even-A chromium isotopes. Calculated spectra, static moments, transition strengths $B(E2)$ and $B(M1)$. Projected Hartree-Fock model with band mixing, $(fp)^n$ model space, modified Kuo-Brown interaction.]

I. INTRODUCTION

The interest in studying the properties of the fp-shell nuclei is evident from the experimental and theoretical results published in literature in recent years. There is a significant increase in the amount of experimental information with the advent of heavy-ion induced reactions. This, in turn, has revived the interest in the theoretical studies of the structure of these nuclei. The early theoretical investigations on the structure of fp-shell nuclei were carried out in the framework of the spherical shell model[1] and the phenomenological deformed rotor-particle coupling (RPC) model.[2] The restricted shell model calculations[1] in a pure $(f_{7/2})^n$ configuration were able to account for a large amount of the then available experimental data on many fp-shell nuclei up to ^{56}Ni. The results of the empirical $(f_{7/2})^n$ shell model with various effective nucleon-nucleon (NN) interactions were published recently.[3] It is, however, quite obvious that the static and dynamic properties of many of the observed nuclear states cannot be described in terms of such restricted shell model calculations. The extension of the shell model configuration space to include the full fp shell has led to a significant improvement[4,5] in correlating the observed properties of the nuclei with $A \lesssim 44$. Owing to the inherent complexities of the shell model calculations in a large configuration space of the full fp shell, such calculations have not so far been reported for nuclei with $A > 44$. However, in view of the substantial pileup of the experimental data, particularly on the high-spin states populated in heavy-ion reactions, it is appropriate to make a systematic study of these nuclei employing a realistic NN interaction in a large configuration space of the complete fp shell. The nuclear eigenstates are generated using the band mixed Hartree-Fock (HF) model which has been used[6,7] with success in vanadium and scandium isotopes. The low-lying eigenstates of nuclei are assumed to be spanned by states of

Entropy production in high energy collisions

G. Bertsch
Physics Department, Michigan State University, East Lansing, Michigan 48824
and Institute for Theoretical Physics, University of California, Santa Barbara, California 93106

J. Cugnon
Institut de Physique, Université de Liège, Liège, Belgium

(Received 29 June 1981)

The entropy production in high-energy collisions is computed in a Monte Carlo cascade model. For collisions of ^{40}Ca on ^{40}Ca at 800 MeV/nucleon beam energy, the computed entropy is 4.4 per particle, about a unit higher than estimated from bulk dynamics. The particle correlation function of the final state is also computed, and is found to be in reasonable accord with a thermal distribution of the same entropy. With such low entropy values, most of the particles emerge in clusters, contrary to experiment. Thus the cascade calculation supports the conclusion of Siemens and Kapusta, that additional degrees of freedom become accessible in heavy ion collisions, beyond those in a conventional nuclear description.

[NUCLEAR REACTIONS ^{40}Ca (^{40}Ca, light composites), $E=800$ MeV/nucleon; calculated entropy, deuteron production, final state clustering.]

I. INTRODUCTION

There is a close connection between deuteron production in high energy heavy ion collisions and the entropy generated in the collisions, pointed out by Siemens and Kapusta.[1] These authors also made the provocative claim that the generated entropy is larger than can be understood with conventional models of the dynamics of nuclear matter. However, this result relies on the validity of a macroscopic treatment of the dynamics, ignoring size effects due to the finite mean free path of the nucleons. In this paper we study the entropy generation and deuteron formation in a finite system using a Monte Carlo cascade model. We do find that additional entropy is produced in a finite system, compared to the bulk value. Nevertheless, the predicted entropy is much lower than the empirical data on deuteron emission suggests.

We begin with the definition of entropy in a system of noninteracting fermions,

$$S=-\int d\gamma[f\ln f+(1-f)\ln(1-f)]\,. \tag{1}$$

Here f is the occupation probability of phase space, and $d\gamma$ is the phase space volume element,

$$\int d\gamma=4\int\frac{d^3r\,d^3p}{(2\pi\hbar)^3}\,. \tag{2}$$

The spin-isospin degrees of freedom give rise to the factor of 4 in Eq. (2). We shall consider only the dilute limit of Eq. (1), $f<<1$, which will be justified later. Then $\ln(1-f)$ may be expanded and Eq. (1) reduces to the classical equation for the entropy,

$$S=A-\int d\gamma\ln f=A(1-\langle\ln f\rangle)\,, \tag{3}$$

where A is the number of particles. As a practical matter, f will be computed in the cascade model by counting particles in cells of phase space. The optimum choice of cell configuration requires some numerical analysis, which we discuss in Sec. II. The heavy ion collision we consider is ^{40}Ca on ^{40}Ca at 800 MeV per nucleon bombarding energy. The actual details of the entropy computation are presented in Sec. III. For the cascade calculations,

Production of 6.13-MeV gamma rays from the $^{16}O(p,p'\gamma)^{16}O$ reaction at 23.7 and 44.6 MeV

J. Narayanaswamy, P. Dyer, S. R. Faber,* and Sam M. Austin
Cyclotron Laboratory and Physics Department, Michigan State University, East Lansing, Michigan 48824
(Received 20 August 1981)

We have measured the cross sections for production of the astrophysically prominent 6.13-MeV gamma ray from the $^{16}O(p,p'\gamma)^{16}O$ reaction at $E^p_{lab} = 23.7$ and 44.6 MeV to be 58.9 and 40.4 mb, respectively. Our results are compared to earlier measurements.

[NUCLEAR REACTIONS $^{16}O(p,p'\gamma)$ ^{16}O. $E = 23.7$ and 44.6 MeV. Measured gamma-ray angular distributions and production cross sections. Implications for gamma-ray astronomy.]

The interpretation of astrophysical gamma-ray line spectra requires the gamma-ray production cross sections and Doppler broadened line shapes for proton and alpha induced reactions over a broad range of projectile energies.[1-4] One can, in principle, calculate the gamma production cross section from inelastic proton and alpha scattering data and gamma-ray branching ratios. However, because of the uncertainties in the contribution of cascade processes to gamma-ray production and the uncertainties in calculating the broadening effects, it is desirable to measure the gamma-ray yields directly. Unfortunately, only a few direct measurements are available for astrophysically abundant nuclei such as ^{12}C, ^{16}O, and ^{56}Fe, and the results are sometimes inconsistent.[1-5] This paper reports a direct measurement for 6.13-MeV gamma rays from the reaction $^{16}O(p,p'\gamma)^{16}O$ at incident lab proton energies of 23.7 and 44.6 MeV. This 6.13-MeV line is one of the most prominent lines in astrophysical gamma-ray line spectra. Our results agree at the lower energy with the cross sections of Dyer *et al.*,[1] but disagree with those of Zobel *et al.*[5]

Protons from the Michigan State University sector-focused cyclotron bombarded a gas target of oxygen, and the resulting gamma rays were detected with two Ge(Li) spectrometers. The natural O_2 target at one atmosphere of pressure was contained in a 3.8 cm diameter aluminum cell with 25μm thick Kapton windows. The increase in the cell diameter when it was filled with gas was found to be 4%, and was taken into account. Beam current, typically 5 nA, was integrated downstream of the gas cell. The beam energy was determined to $\pm 0.1\%$ by magnetic analysis. Average beam energies within the target were 23.66 and 44.61 MeV, for the two cases.

The smaller detector (nominal efficiency 9%) was kept fixed in position to monitor gamma rays from the target. The larger detector (nominal efficiency 16%) was mounted on a goniometer arm about 32 cm from the target. A lead absorber 1 mm thick was placed in front of the larger detector to reduce the counting rate from x rays and low-energy gamma rays. At 6.13 MeV, the detector resolution was about 15 keV, but most peaks were much wider due to Doppler broadening. Count rates were typically 5000 counts/sec. For determining dead times (about 15%), signals from the monitor detector were used to trigger a pulser which fed the preamplifier of the larger detector and a scaler.

The 6.13-MeV line arises from $E3$ transition, and determination of total cross section, therefore, requires measurements at at least three angles. Measurements were made at several angles between 45° and 157° relative to the incident beam direction. At each angle, data were acquired with the cell filled with gas and with the cell empty, typical counting times being 90 and 45 min, respectively. Energy spectra were recorded with a Sigma 7 computer. Detector efficiency was measured with a calibrated source[6,7] of 6.13-MeV gamma rays (^{238}Pu + ^{13}C) in the same source-detector geometry as that of the experimental runs.

Typical spectra (after subtracting the cell contribution) are shown in Fig. 1. The analysis was complicated by the overlap of the broad 6.13-MeV full energy peak (FEP) with the double escape peak (DEP) of the 7.12-MeV line from ^{16}O, at 6.10 MeV. The latter peak (about 10% of the total area) had to be subtracted before extracting the

Reinterpretation of the $^2H(d,pp)nn$ reaction at 80 MeV

Robert E. Warner*
Cyclotron Laboratory, Michigan State University, East Lansing, Michigan 48824
(Received 10 August 1981)

Leeman *et al.* measured $^2H(d,pp)nn$ cross sections at 80 MeV. They interpreted their results in terms of double spectator processes and had limited success in fitting their spectra. We obtain good fits to all their reported data by assuming final-state interactions between both final n-p pairs and ignoring the double spectator process.

[NUCLEAR REACTIONS $^2H(d,pp)nn$, $E=80$ MeV; calculated $\sigma(E_1E_2,\theta_1,\theta_2)$ assuming n-p final-state interactions. Improved fits over original interpretation assuming double spectator process.]

Leeman *et al.*[1] have searched for the double spectator process (DSP) in the $^2H(d,pp)nn$ reaction at 80 MeV. They observed proton-proton coincidences under conditions where the neutron from the target could (but did not necessarily) remain at rest in the lab while the other neutron maintained the projectile velocity. Their plane-wave Born approximation (PWBA) calculations based on the DSP imperfectly reproduced the data, and they speculated that formation of two singlet deuterons contributed to the observed yield at one geometry.

In contrast, I obtain good fits to all their reported data by assuming final-state interactions (FSI) between both final n-p pairs and ignoring the DSP. Both the Wigner and the $V_{\sigma\tau}$ components of the nucleon-nucleon force can cause double breakup, and so the four-body final state is assumed to be an incoherent mixture of two $^1S_0$ (singlet deuteron) and two $^3S_1$ n-p pairs.

The geometry of the experiment is shown in Fig. 1. Two protons are detected with equal lab energies E at equal coplanar lab angles θ. The n-n center-of-mass (c.m) velocity $\vec{V}_{nn}$ and the magnitudes of the n-n relative velocities $\vec{V}_3'$ and $\vec{V}_4'$ are then determined. But the n-n emission angles α,ϕ in the n-n c.m. frame are completely undetermined and predictions must be integrated over α and ϕ.

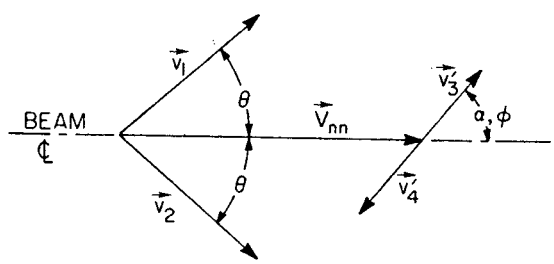

FIG. 1. Geometry for $^2H(d,pp)nn$ reaction.

Watson and Migdal[2,3] have shown that, when a final-state n-p pair have small enough relative momentum $\hbar k$, their wave function may be written

$$\psi_{np}=\frac{e^{-i\delta}\sin\delta}{k}f(r)\,, \tag{1}$$

where δ is the elastic scattering phase shift and r is their separation. Thus, the square modulus of our matrix element contains a factor $(\sin^2\delta/k^2)$ for each n-p pair which, at relevant k's, is larger for the $^1S_0$ state. Therefore, the yield $Y(E,\theta)$ is given by

$$Y(E,\theta)=A\int\left\{\left[\frac{\sin^2\delta_1}{k^2}\right]_L\left[\frac{\sin^2\delta_1}{k^2}\right]_R+\eta\left[\frac{\sin^2\delta_3}{k^2}\right]_L\left[\frac{\sin^2\delta_3}{k^2}\right]_R\right\}\times\rho_F\sin\alpha\,d\alpha\,d\phi\,, \tag{2}$$

where ρ_F is the density of final states. The subscript $L(R)$ designates the proton detected on the left (right) of the beam and the neutron emitted nearest to it. The singlet and triplet n-p phase shifts δ_1 and δ_3 were calculated from the effective range parameters of Guratzsch *et al.*.[4] The normalization A and triplet-to-singlet ratio η were the only parameters adjusted while fitting 48 data points. The units used in Eq. (2) for $Y(E,\theta)$,

PHYSICAL REVIEW C VOLUME 25, NUMBER 1 JANUARY 1982

Production of ^{6}He, ^{6}Li, ^{7}Li, and ^{7}Be in the $\alpha+\alpha$ reaction between 60–160 MeV

B. G. Glagola
Chemistry Division, Argonne National Laboratory, Argonne, Illinois 60439

V. E. Viola, Jr.
Chemistry Department and Cyclotron Facility, Indiana University, Bloomington, Indiana 47405

H. Breuer, N. S. Chant, A. Nadasen, and P. G. Roos
Physics Department, University of Maryland, College Park, Maryland 20742

Sam M. Austin
Department of Physics and Cyclotron Laboratory, Michigan State University, East Lansing, Michigan 48824

G. J. Mathews
Lawrence Livermore Laboratory, Livermore, California 94550
(Received 13 July 1981)

Cross sections for the production of ^{6}He, ^{6}Li, ^{7}Li, and ^{7}Be produced in the $\alpha+\alpha$ reaction have been measured over the energy range 60–160 MeV. Detailed angular distributions are presented for exit channels leading to ^{7}Li, ^{7}Be, and ^{6}Li(g.s.), along with cross sections for the three-body exit channels leading to the production of ^{6}He and ^{6}Li. The astrophysical significance of the $\alpha+\alpha$ reaction is discussed with particular emphasis on the production of ^{7}Li in the interaction of galactic cosmic rays with the interstellar medium. In addition, two-nucleon-transfer distorted-wave Born approximation calculations are presented in an attempt to understand the reaction mechanism operating in the $\alpha(\alpha,d)^6$Li(g.s.) reaction.

[NUCLEAR REACTIONS ^{4}He(^{4}He,HI), HI=^{6}He, ^{6}Li, ^{7}Li, and ^{7}Be; $E=60-160$ MeV; measured $d^2\sigma/d\Omega\,dE$ and $\sigma(E)$; astrophysical relevance discussed; DWBA calculations for ^{4}He(^{4}He,d)^{6}Li.]

I. INTRODUCTION

The $\alpha+\alpha$ reaction is well known to play an important role in the nucleosynthesis of nature's elements.[1] At the sub-Coulomb energies characteristic of stellar interiors, the $\alpha+\alpha\rightarrow[\mathrm{Be}^8]^*$ reaction provides the critical intermediate step in the 3α reaction which leads to the formation of ^{12}C and heavier elements. At higher energies $\alpha+\alpha$ collisions contribute significantly to the abundance of the light element Li via cosmic-ray-like processes. Although the abundance of Li (as well as Be and B) is very low, studies of its origin have important implications on our understanding of the universe.

While big bang nucleosynthesis can account for most of the H and He in the universe[2] and stellar evolution cycles are believed to produce ^{12}C and heavier nuclei,[1] the synthesis of Li, Be, and B (LiBeB) requires additional mechanisms. Calculations indicate that ^{7}Li may be produced in meaningful abundances in the big bang, but the predicted yields for ^{6}Li, ^{9}Be, ^{10}B, and ^{11}B are far below the observed values.[2] In the dense, hot environments associated with stellar evolution LiBeB are usually destroyed,[3] which implies that these elements must have their origin in dynamic, nonequilibrium processes. Accordingly, the abundances of LiBeB serve as a valuable indicator of the properties of such phenomena.

One of the most probable mechanisms for production of LiBeB is the interaction of galactic cosmic rays (GCR) with the interstellar medium.[3,4] This mechanism reproduces the measured abundances of ^{6}Li, ^{9}Be, ^{10}B, and ^{11}B relatively well. However, attempts to account for ^{7}Li via the GCR mechanism result in an underproduction of this

ϵ/β^+ decay of ^{145}Gd: Resolution of ϵ/β^+ decay branching ratio anomalies and evidence for pronounced structures in the β-decay strength

R. B. Firestone,* R. C. Pardo,† R. A. Warner,‡ Wm. C. McHarris, and W. H. Kelly§
National Superconducting Cyclotron Laboratory and Departments of Chemistry and Physics, Michigan State University, East Lansing, Michigan 48824
(Received 23 March 1981)

The ϵ/β^+ decay of 23.0-min ^{145}Gd has been thoroughly studied with Ge(Li) and plastic scintillator detectors. A total of 326 γ rays deexciting 136 levels in ^{145}Eu have been placed by this work. The available decay energy, $Q_\epsilon = 5.07 \pm 0.06$ MeV, was measured by β-γ coincidence techniques. ϵ/β^+-decay branching ratios have been measured for several transitions, and a long standing anomaly in those ratios has been resolved by the new Q_ϵ value and the discovery of additional electron-capture decay. We have investigated the β-strength function for ^{145}Gd and discovered pronounced structure with resonances at 1042, 1819, 2584, and 4500 keV. The 1042-keV resonance is proposed to result from a $(\pi d_{3/2})^2(\nu s_{1/2})^{-1} \rightarrow (\pi d_{3/2})^1$ β transition, the 1919- and 2584-keV resonances from $(\pi d_{5/2})^2 \rightarrow [(\pi d_{5/2}) \otimes 2^+]_{1,2}$ decays, and the very strong 4500-keV resonance from the $(\pi h_{11/2})^2 \rightarrow (\pi h_{11/2}) \otimes (\nu h_{9/2} + \nu f_{7/2} + \cdots)$ transition across the shell closure.

[RADIOACTIVITY ^{145}Gd; measured E_γ, γ-γ coin, E_β, β-γ coin, Q, $t_{1/2}$, x-γ coin, $\gamma^{\pm}$-γ coin; deduced ϵ/β^+ ratios, logft, β-strength function, missing continuum decay intensity. ^{145}Eu; deduced levels, J, π; calculated level energies with shell model, weak-coupling model.]

I. INTRODUCTION

Since ^{145}Gd[g] was first characterized in 1959 by Grover[1] and later by Olkowsky *et al.*,[2] it has continued to spark considerable interest and controversy. This decay is uncharacteristic when compared with the lighter $N = 81$ odd-A isotones. Despite having much greater available decay energy, ^{145}Gd (in this paper ^{145}Gd will be taken to mean ^{145}Gd[g] unless stated otherwise) is more than twice as long lived as ^{143}Sm and displays a completely different decay pattern.

In 1970 Newman *et al.*[3] reported spins and parities for a number of the low-lying states in the ^{145}Eu daughter determined by the ^{144}Sm$(\tau,d)^{145}$Eu reaction, and they also reported the analysis of a high-resolution Ge(Li) γ-ray spectrum associated with ^{145}Gd decay.

In 1971 Eppley, McHarris, and Kelly[4] presented a more complete decay scheme for ^{145}Gd that explained many of its decay properties. They showed that the unique ^{145}Gd decay pattern resulted partly from the crossing of the $\nu s_{1/2}$ state below the $\nu d_{3/2}$ state to become the ground state in ^{145}Gd. This effectively blocked all simple allowed β transitions between available shell-model states and forced the decay to proceed primarily to high-lying states of more complex character.

Although Eppley, McHarris, and Kelly resolved one controversy, they opened up another, more perplexing question. In the course of their decay-scheme studies, they measured ϵ/β^+-decay branching ratios (hereafter referred to as ϵ/β^+) for the stronger β transitions from ^{145}Gd. Some of these values deviated significantly from allowed β-decay theory and could not be explained at that time. Firestone *et al.*[5,6] pursued this question in 1974 and 1975 in a series of progressively more precise experiments; yet the ϵ/β^+ anomalies persisted. They proposed[7] that the inclusion of second-order corrections to the allowed theory of ϵ/β^+ ratios might produce such anomalies in *hindered* allowed decays, but, as this suggestion could not be experimentally verified for the complex ^{145}Gd decay, the matter remained in question.

In 1976 Firestone *et al.*[8] reported a more complete Ge(Li) γ-ray singles spectrum for ^{145}Gd taken with a larger detector than had been previously

Forward-angle inelastic scattering

G. F. Bertsch and O. Scholten
Cyclotron Laboratory, Michigan State University, East Lansing, Michigan 48824
and Institute for Theoretical Physics, University of California at Santa Barbara, Santa Barbara, California 93106
(Received 28 September 1981)

The single-step contribution to nuclear inelastic scattering is analyzed in the independent particle model. We derive simple formulas for the single-step total cross section and the response function, which are the two major ingredients in the theory. This description accounts for most of the cross section below an excitation energy of 40 MeV, seen in proton induced reactions at 200 and 800 MeV.

[NUCLEAR REACTIONS Calculated proton induced one step continuum $\sigma(E,E_p)$, $q(E,E_n)$, $\sigma(\theta)$ at 200 and 800 MeV protons.]

I. INTRODUCTION

Inelastic scattering reactions are particularly interesting at forward angles because the low momentum transfer probes the collective response of nuclei to external fields. However, the collective cross section is obscured by a background which we would like to understand better. One question is whether this background arises primarily from single or multiple collisions. In this work we will examine the single step contribution to the cross section. We consider the regime of excitation energies below 40 MeV in proton-induced reactions with proton energy greater than 200 MeV, and we will show that the single step contribution accounts for most of the cross section at momentum transfers larger than 0.5 fm^{-1}. The inclusive inelastic scattering has been previously studied by Chiang and Hüfner.[1] Our approach is similar in spirit to this work.

The theory of the cross section will be based on the distorted-wave impulse approximation which allows the nucleon-nucleon cross section to be factorized from the nuclear response.[2] We express the cross section in the form

$$\frac{d^2\sigma}{d\Omega\, dE} = \frac{d\sigma}{d\Omega}\bigg|_{NN} N_{\text{eff}} S(q,E) \,. \tag{1.1}$$

Here $d\sigma/d\Omega\,|_{NN}$ is the nucleon-nucleon cross section at the same laboratory energy and angle. The second factor in this equation, N_{eff}, is the effective number of target particles which will be discussed in Sec. II. The nuclear response to the projectile scattering probe is $S(q,E)$. This is defined by

$$S(q,E) = \frac{\sum_{i,f} \langle \psi_i \mid \mathcal{O}_q \mid \psi_f \rangle^2 \delta(E_f - E_i - E)}{\sum_i \langle \psi_i \mid \mathcal{O}_q^\dagger \mathcal{O}_q \mid \psi_i \rangle} \,, \tag{1.2}$$

where $\mathcal{O}_q$ is the projectile scattering operator, and ψ_i and ψ_f are occupied and unoccupied single-particle states. Note that in the limit that $\mathcal{O}_q \mid \psi_i\rangle$ orthogonal to all the $\mid \psi_{i'}\rangle$ (no Pauli blocking), S satisfies

$$\int dE\, S(q,E) = 1 \,. \tag{1.3}$$

We discuss the theory of $S(q,E)$ in Secs. III and IV. In Sec. III we review the Fermi gas model for the response, which is used in Ref. 1. Our main interest is the small momentum transfers, which requires a better treatment of the nuclear surface than is possible in the Fermi gas model. We present the theory of S in a semi-infinite slab model in Sec. IV. Finally, in Sec. V we present a detailed comparison of these models with proton-induced reactions at 200 and 800 MeV.

II. SINGLE STEP TOTAL CROSS SECTION

We define the cross section $\sigma^{(n)}$ for n collisions between projectile and target particles in the nucleus. The effective number of nucleons participat-

PHYSICAL REVIEW C VOLUME 25, NUMBER 4 APRIL 1982

Role of isobar-hole excitations in the quenching of the $^{40}K(\beta^-)^{40}Ca$ transition

B. Castel
Oak Ridge National Laboratory, Oak Ridge, Tennessee 37830
and Physics Department, Queen's University, Kingston, Canada K7L 3N6*

H. Toki
Cyclotron Laboratory, Michigan State University, East Lansing, Michigan 48824

P. Blunden
Physics Department, Queen's University, Kingston, Canada K7L 3N6
(Received 2 November 1981)

The quenching effects of nuclear and Δ excitations on the β decay of ^{40}K are examined. It is found that although configuration mixing still provides the largest retardation, the inclusion of isobar-hole excitation is necessary to bring the calculation within calling distance of the experimental decay rate.

[RADIOACTIVITY $^{40}K(\beta^-)^{40}Ca$. Shell model calculation including isobar-hole excitations.]

The existence of collective magnetic states, long speculated as the reason for depletion of magnetic strength in low lying states, is beginning to emerge as a question of fundamental importance in nuclear spectroscopy. In both γ and β decays involving spin operators a mass dependent quenching has been observed and several mechanisms have been invoked as possible contributors. In this paper, we examine in detail the influence of the nuclear and Δ-coupling mechanisms as they relate to an example of retarded β decay rate whose hindrance remains not fully understood more than 10 years after its experimental determination.

The β decay branch of ^{40}K $(4^-, T=1)$ to the ground state of ^{40}Ca $(0^+, T=0)$ was first determined by Warburton *et al.*[1] in 1970 as corresponding to a unique third forbidden transition retarded by about 5 times compared to the single particle (s.p.) estimate.[2] The transition is essentially a one-particle–one-hole transition corresponding to the spin part of an $M4$ γ decay operator. A few years ago Towner[2] investigated this particular decay rate using an extended version of the schematic model and traced the hindrance to the repulsive nature of the $T=1$ particle-hole force resulting in the formation of a giant $M4$ resonance with a rather broad distribution. Using a realistic set of two body parameters, Towner found that although the collective $M4$ state exhausted a large fraction of the sum rule, the calculated β decay of the lowest 4^-, $T=1$ state was still much larger than experiment. Following Warburton *et al.*[1] we have calculated the third forbidden β decay by expanding the one-particle–one-hole space for ^{40}K to include all $2s$-$1d$ and $1f$-$2p$ particle-hole states. The ^{40}K ground state is constructed by diagonalizing an effective two body interaction in this space. Both results using the Gillet-Sanderson[3] and the Perez[4] interaction indicate that although ^{40}K is seen to be more than 98% pure $f_{7/2} - d_{3/2}^{-1}$, the remaining configurations, although small, have all coefficients which are out of phase with the leading terms. These small terms yield nonzero overlap with the 2p-2h configuration of the ^{40}Ca g.s. and their net effect on the β decay moment is, as shown on Fig. 1, to reduce the transition rate by nearly half (52%). To come closer to experiment,

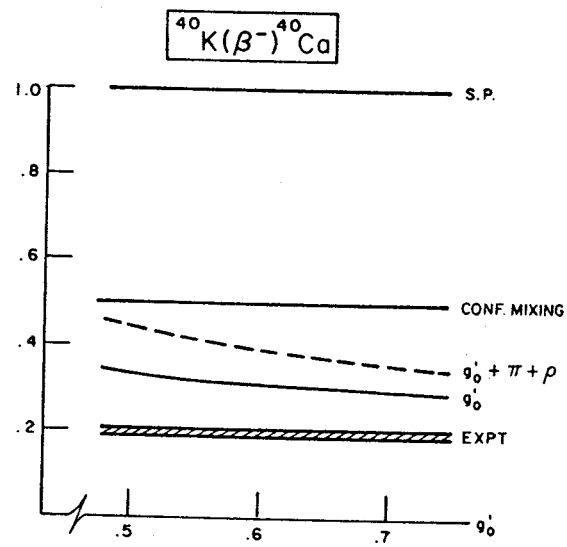

FIG. 1. The $4^- \rightarrow 0^+$ decay rate, in single particle units, displayed as a function of the p-h coefficient g_0'.

Hadronization by color bremsstrahlung

J. F. Gunion* and G. Bertsch†
Institute for Theoretical Physics, University of California, Santa Barbara, California 93106
(Received 20 July 1981)

Particle production in the central plateau of hadronic final states is calculated in a perturbative QCD model. We assume that the controlling process is bremsstrahlung of gluons. We find important differences between the spectrum produced in soft hadronic collisions and the spectrum in e^+e^- annihilation. Describing soft hadronic collisions with the Low-Nussinov model, we find that the central plateau is independent of total energy, but depends strongly on the momentum transfer in the soft-gluon exchange. In contrast, the quark jets from e^+e^- annihilation have a central plateau growing with energy. The strong momentum dependence in the hadron-induced plateau arises from the cancellations in the amplitude associated with the gauge invariance of the theory.

I. INTRODUCTION

In perturbative quantum chromodynamics (QCD) the evolution of color jets in hard interactions is a sequential process, describable by classes of Feynman diagrams as in the jet calculus.[1] For example in e^+e^- annihilation, the particle production is initiated by perturbatively produced radiation which begins immediately after the creation of the q and $\bar{q}$ jets. Eventually the nonperturbative confinement aspects of QCD become dominant and the radiation products materialize as hadrons. Nevertheless in this description it is the underlying perturbatively produced color quanta which largely determine the distribution and multiplicity of final-state particles.

Whether or not such ideas are applicable to hadron-hadron collisions has been a subject of continuing debate. At currently available energies, the experimental multiplicities of hadron-hadron and e^+e^- final states are about the same. Theoretically, the mechanism behind this universality is not apparent. We will investigate this question in the context of the Low-Nussinov model for hadron-hadron interactions.[2] In this model the constant total cross section arises from the exchange of a gluon between quarks in the colliding hadrons, as in Fig. 1. After this gluon exchange, the state consists of two rapidly separating color octets, analogous to the separating q and $\bar{q}$ color triplets produced by e^+e^- annihilation, as in Fig. 2(a). In both cases the color separation will lead to bremsstrahlung radiation. The relationship between the final states will depend upon the relative distribution of radiation products in the two cases.

We present results here for this comparison at the simplest level—lowest-order perturbation theory with one radiated gluon. We focus on the central plateau region. In e^+e^- annihilation, the calculation is quite easy. At high energy, and in an appropriate gauge, there is only one diagram to compute, Fig. 2(b). For the case of hadron collisions, we must consider all diagrams, to a given order in the coupling constant, to arrive at a gauge-invariant result. The important diagrams

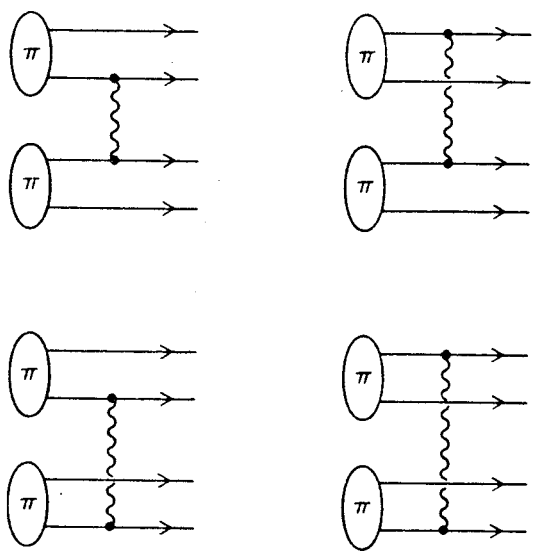

FIG. 1. Feynman diagrams for the total hadron-hadron cross section in the Low-Nussinov, gluon-exchange model.

Nuclear Physics A365 (1981) 61–92

ROTATIONAL BANDS IN ^{170}Yb OBSERVED FOLLOWING (α, xn) REACTIONS

P. M. WALKER

*Science Research Council, Daresbury Laboratory, Daresbury, Warrington WA4 4AD, UK**

and

Cyclotron Laboratory, Michigan State University, East Lansing, Michigan 48824, USA

W. H. BENTLEY, S. R. FABER †, R. M. RONNINGEN and R. B. FIRESTONE ‡

Departments of Physics & Chemistry and Cyclotron Laboratory, Michigan State University, East Lansing, Michigan 48824, USA

F. M. BERNTHAL

*Departments of Chemistry and Physics and Cyclotron Laboratory, Michigan State University, East Lansing, Michigan 48824, USA**

and

Niels Bohr Institute, Risø, DK-4000 Roskilde, Denmark

and

J. BORGGREEN, J. PEDERSEN and G. SLETTEN

Niels Bohr Institute, Risø, DK-4000 Roskilde, Denmark

Received 11 November 1980
(Revised 11 March 1981)

Abstract: At least seven side bands, with $K^\pi = (0^+), (1^-), (2^+), (3^-), 4^-, 6^-$, and 7^-, have been identified in ^{170}Yb up to high spin, using γ-ray techniques following (α, 2n) and (α, 4n) reactions. Backbending in the positive-parity yrast band is confirmed, and candidates for low-spin members of the S-band are found. The negative-parity yrast band has behaviour characteristic of both strong coupling and decoupling. These properties, together with those in the other negative-parity side bands, are interpreted as arising from Coriolis effects on the quasiparticle configurations, and the experimental results are compared with a two-quasiparticle-plus-rotor calculation. Evidence of $\Delta K = 2$ mixing is found in the $K = (3)$ side band. The relationship between the moments of inertia of the positive-parity and negative-parity yrast bands in the $N = 100$ isotones is discussed in the framework of a simple empirical model, giving insight into the presence or absence of backbending. The negative-parity yrast bands in the $N = 100$ isotones are compared. Their significant differences are qualitatively reproduced in two-quasiparticle-plus-rotor calculations.

E NUCLEAR REACTIONS ^{168}Er(α, 2n), $E = 27$ MeV; ^{170}Er(α, 4n), $E = 50$ MeV: measured E_γ, I_γ, $\gamma\gamma$-coin, α-$\gamma(t)$, $\gamma(\theta)$, ICC. ^{170}Yb deduced levels, $K, J, \pi, T_{1/2}$. Ge, Ge(Li), Si(Li) detectors, enriched targets.

* Present address.

† Present address: Argonne National Laboratory, Argonne, Illinois 60439, USA.

‡ Present address: Lawrence Berkeley Laboratory, University of California, Berkeley, California 94720, USA.

Nuclear Physics A380 (1982) 509–528

DESCRIPTION OF THE EUROPIUM ISOTOPES IN THE INTERACTING BOSON-FERMION MODEL

O. SCHOLTEN

Cyclotron Laboratory, Michigan State University, East Lansing, Michigan 48824 *
and
Kernfysisch Versneller Instituut, Groningen, The Netherlands

and

N. BLASI

Kernfysisch Versneller Instituut, Groningen, The Netherlands

Received 19 October 1981

Abstract: Properties of the odd-mass Eu isotopes are investigated in the framework of the interacting boson-fermion approximation (IBFA) model. It is shown that in the IBFA model a rather detailed and yet simple description can be given of odd-mass nuclei ranging from spherical ^{147}Eu to deformed ^{155}Eu. Calculated excitation energies, proton separation energies, E2 and M1 transition probabilities, quadrupole and magnetic moments and spectroscopic factors for single-proton transfer are compared with experiment. The model parameters determined are compared with the predictions of a simple microscopic theory.

1. Introduction

To describe heavy odd-mass nuclei ($A > 100$) various models have been developed. The majority of these are based on a particle-core coupling scheme. Spherical nuclei can be treated in terms of the weak-coupling limit of particle-vibration models [1]. An accurate description of well-deformed nuclei can be obtained in terms of the Nilsson scheme [1]) or other geometrical models [2]). In their respective limiting situations these models can describe the properties of odd-mass nuclei. A description of intermediate cases, the so-called transitional nuclei, would involve lengthy and complicated calculations and has so far only been done for even-even nuclei [3]).

In the IBFA model [4]) odd-A nuclei are described by coupling the degrees of freedom of the odd particle to a core which is given in terms of the IBA model [5–7]). The IBA model gives a simple unified description of vibrational [5]), rotational [6]) γ-unstable [7]) as well as transitional [8, 9]) even-even nuclei. It has also been shown [10, 11]) that for the limiting cases the results of the IBFA model are comparable to those of the conventional models [1]). By applying the model to the europium (Eu) isotopes it is shown that transitional nuclei can also be described.

* Present address.

Nuclear Instruments and Methods 189 (1981) 351–356
North-Holland Publishing Company

A SURFACE IONIZATION SOURCE FOR BEAM ENERGY CALIBRATION

P. DYER and R.G.H. ROBERTSON
Cyclotron Laboratory and Department of Physics, Michigan State University, East Lansing, Michigan 48824, U.S.A.

Received 10 February 1981

A surface ionization source has been constructed to produce Tl^+ ions having the same magnetic rigidity as light ions of a few MeV energy. The light-ion energy is determined by matching the paths of the light and Tl^+ ions through a magnetic spectrometer and by measuring the source voltage with a precision voltage divider and voltmeter. The absolute calibration has been verified by measuring the energy of alpha particles from a ^{212}Bi source and by measuring the $^{14}N(p, n)^{14}O$ reaction threshold.

1. Introduction

In the attempt to measure hadronic neutral current parity violation in the inverse alpha decay of the 3.563 MeV, 0^+ state of ^6Li, we search for a resonance in the $^2H(\alpha, \gamma)^6Li$ reaction at $E_\alpha = 6.238$ MeV (lab energy) [1]. It is required that the beam energy be known with an absolute accuracy of about 2 parts in 10^4 and that it be possible to match the beam energy from one data acquisition period to the next with an accuracy of 1 part in 10^4. In order to eliminate the uncertainties in the calibration of the accelerator beam analyzing magnet, especially those involved in interpolating or extrapolating calibration measurements at other energies, we have designed a system with which we can frequently (and with little effort) measure the energy of the beam at the $^2H(\alpha, \gamma)^6Li$ resonance energy.

For this purpose we built a surface ionization source. The source, operating at 30.47 kV, produced Tl^+ ions of the same magnetic rigidity as the 6.238 MeV α^{++} beam. Both beams could be brought down the beam line and through a Q3D spectrometer [2] to the focal plane, where the beam energy was measured by matching currents on the two halves of a split Faraday cup and measuring the voltage applied to the source extraction electrode with an accuracy of 0.01%.

The source is described in section 2, the procedure for its use is given in section 3, and two measurements for checking the absolute accuracy are given in section 4 (^{212}Bi source alpha particle energy measurements) and section 5 [$^{14}N(p, n)^{14}O$ threshold measurement]. A summary is given in section 6. All measurements described here were made at the Chalk River Nuclear Laboratory (CRNL), with the exception of the α source calibration, which was done at the Michigan State University (MSU) Cyclotron Laboratory. The description is that of the Chalk River configuration, unless otherwise noted.

Similar work has been carried out independently at the University of Auckland [3,4].

2. Description of the ion source

In the surface ionization process, an atom of low ionization potential (in our case thallium, $V_i = 6.1$ eV) is ionized by contact with a surface of high work function (in our case iridium, $\phi = 5.3$ eV) which is hot enough to thermally desorb the ion. Because of the surface nature of the interaction and the equipotential maintained by the metallic ionizer, the kinetic energy of the ions is determined by the voltage applied to the ionizer. (The kinetic energies for zero applied voltage have a Maxwellian distribution characteristic of the temperature of the ionizer; in our case $\frac{3}{2}kT$ is 10^{-5} times the applied voltage.) Thallium was chosen because it is relatively heavy (not requiring very high voltages for an ion of a given magnetic rigidity), has a relatively low ionization potential, and is easily evaporated to form an atomic beam. To match the rigidity of 6.24 MeV α^{++} particles, a voltage of 30.5 kV was required.

The ion source was mounted on a water-cooled copper flange and was housed in an O-ring-sealed

0029-554X/81/0000–0000/$02.50

Nuclear Instruments and Methods 193 (1982) 557–561
North-Holland Publishing Company

IMPROVEMENT OF TIME RESULUTION OF COAXIAL Ge(Li) DETECTORS BY TIME WALK CORRECTION

J. KASAGI *, H. OHNUMA
Department of Physics, Tokyo Institute of Technology, Meguro-ku, Tokyo, Japan

and

N. OHYAMA
Image Science and Engineering Laboratory, Tokyo Institute of Technology, Nagatsuta, Midori-ku, Yokohama, Japan

Received 29 January 1981 and in revised form 24 July 1981

A technique to correct the time walk due to the rise-time change has been developed in order to improve the time resolution of coaxial Ge(Li) detectors. Typical time resolutions (fwhm) of 2.0 ns for 1332 keV gamma rays and 3.4 ns for 511 keV gamma rays have been obtained for a 60 cm^3 coaxial Ge(Li) detector. It is emphasized that the improvement can be achieved without any loss of efficiency.

1. Introduction

It is well known that the charge collection time of a coaxial Ge(Li) detector is not constant but depends on the details of the interactions within the crystal producing a particular pulse. This variation is reflected in the pulse-shape change at preamplifier and fast amplifier outputs. Timing discriminators introduced to improve the time resolution [1,2] usually compensate the time walk due to the pulse-height change, but the time walk due to the pulse-shape change is poorly compensated by these discriminators. The time resolution of large coaxial Ge(Li) detectors, therefore, is mainly limited by this variation in pulse shapes.

Much improved time resolution of coaxial Ge(Li) detectors has been obtained by White and McDonald [3], using a pulse-shape discrimination technique with a dual constant fraction discriminator. Their result shows the possibility of improving the time resolution by selecting pulses with a certain rise-time. However, the detection efficiency is inevitably reduced to about 60%.

We have developed a method to improve the time resolution of large coaxial Ge(Li) detectors. The method presented here is to correct the time walk using the correlation between the rise-time and the timing output. It is emphasized that a much improved time resolution can be obtained without any loss in efficiency.

2. Pulse shape considerations

The pulse used for the timing system input depends not only on the manner in which electric charge is collected by the detector electrodes but also depends on the response of an amplifying chain between the detector output and the timing system input. A preamplifier, a timing filter amplifier (TFA) and a constant fraction discriminator (CFD) are used in a conventional setup. Therefore we consider here the pulse shape of the TFA output, assuming that the charge produced by the interaction of a gamma ray with the detector is localized to a point.

Calculated pulse shapes at the TFA output are shown in fig. 1 for different interacting positions. Here R is the radius at which the gamma ray is absorbed. The details of the calculation are described in Appendix. As shown in fig. 1, the rise-time of the TFA output pulse is strongly affected by R. The peak

* Present address: Cyclotron Laboratory, Michigan State University, East Lansing, MI 48824, U.S.A.

0029-554X/82/0000–0000/$02.75

Z. Phys. A - Atoms and Nuclei 305, 131-134 (1982)

Zeitschrift für Physik A Atoms and Nuclei

Angular Momentum, Statistical Equilibrium and Sequential Fission in Very Asymmetric Systems

D.J. Morrissey*, G.J. Wozniak, L.G. Sobotka, A.J. Pacheco**, C.C. Hsu***, R.J. McDonald, and L.G. Moretto
Nuclear Science Division, Lawrence Berkeley Laboratory, University of California, Berkeley, California, USA

Received November 6, 1981

The in- and out-of-plane angular distributions for fission fragments in coincidence with projectile-like products from the reaction of 252 MeV ^{20}Ne with ^{197}Au and ^{238}U have been measured. The results are compared to a statistical model which has successfully explained γ-ray anisotropies from a heavy symmetric system. The agreement is rather good after proper consideration of the direction of the line-of-centers at contact.

The measurement of the internal spin and its alignment for reaction partners from deep-inelastic heavy-ion collisions (DIC) has become an important tool for studying the process of angular momentum transfer. The measurement of fluctuations in the spin components provides a good test of whether statistical equilibrium of the angular momentum bearing modes of the dinuclear complex is achieved in a DIC [1]. Evidence for statistical equilibrium has been observed in symmetric reactions which have been studied by means of γ-ray angular distributions. In the very asymmetric ^{20}Ne+^{197}Au and ^{238}U systems the statistical excitation of a number of angular momentum bearing modes is strongly suppressed. In particular, a large difference in the moments of inertia of the two reaction partners will increase the amount of energy necessary to excite any mode in which the small fragment is forced to rotate (wriggling, bending and twisting) [1-3]. Excitation of the only surviving mode (tilting) predicts a minimum in the angular distribution of sequential fission fragments along the line-of-centers [4]. But the direction of the line connecting the centers of the two nuclei at contact is not generally colinear with the laboratory recoil direction and is dependent on energy loss.

The statistical equilibrium model that we employed has been developed by Moretto and Schmitt [1] and Moretto, Blau and Pacheco [2]. In this model the fixed aligned components of the fragments angular momenta couple to angular momentum components associated with the internal modes of the complex [3] causing the total fragment angular momentum to become misaligned. When the reaction partners have equal masses, the thermal widths of the angular momentum components are nearly equal in cartesian coordinates (x-axis taken along the line-of-centers). However, as one considers partners with progressively different masses, and hence different moments of inertia, the situation changes dramatically [4]. The statistical widths of the angular momentum components in the heavy fragment generated by the normal modes are shown individually in Fig. 1 as a function of mass asymmetry. These widths are projected onto the cartesian coordinates such that $\sigma_x^2=\sigma_{\text{tilt}}^2+\sigma_{\text{twist}}^2$ and $\sigma_y^2=\sigma_z^2=\sigma_{\text{bend}}^2+\sigma_{\text{wrig}}^2$. In general terms, if the angular momentum is predominantly perpendicular to the line-of-centers, an in-plane anisotropy arises when $\sigma_x^2\neq\sigma_y^2$, i.e., at large mass asymmetries ($\sigma_x^2\approx\sigma_{\text{tilt}}^2>\sigma_y^2\approx\sigma_{\text{bend}}^2$). Thus very asymmetric reaction systems should provide an excellent test of the excitation of selected normal modes and of the statistical model in general.

Experimental techniques used to measure the spin and its alignment for DIC products include continuum γ-ray [5, 6], alpha particle [7, 8] and sequential fission fragment [9-12] angular distributions. If one considers only reactions with the *most negative*

* Permanent address: Department of Chemistry and Cyclotron Institute, Michigan State University, East Lansing, Michigan 48824, USA

** Permanent address: Comision Nacional de Energia Atomica, Buenos Aires, Argentina

*** Permanent address: Institute of Atomic Energy, Beijing, China

0340-2193/82/0305/0131/$01.00

McGRAW-HILL ENCYCLOPEDIA OF SCIENCE AND TECHNOLOGY, 5/e (April, 1982)

Spallation reaction

A nuclear reaction in which the interacting nuclei are disintegrated into a large number of the constituent protons, neutrons, and other light particles. Compared to more conventional reactions involving the simple transfer of nucleons between the colliding nuclei, spallation is a violent process occurring at high incident energy. An extreme case is shown in the illustration, the interaction of an argon nucleus (18 protons and 22 neutrons) with a lead nucleus (82 protons and 126 neutrons) in a streamer chamber at an incident energy of 72,000 MeV. The emitted charged particles appear as tracks of electrical discharge in a gas. In this example the nuclei are apparently completely shattered into individual nucleons. Spallation can also be induced by lighter particles, such as high-energy protons; however, these reactions are usually less violent and produce only a few particles (typically 3 to 10). Although the most abundant final products are protons, neutrons, and alpha particles, the spallation of larger fragments such as lithium and carbon also occurs. The short, thick tracks in the illustration are probably created by the emission of these larger fragments of nuclear matter.

The detailed mechanism whereby the incident energy is communicated to the nuclei in the spallation process is not well understood, but there may well be analogies with the breakup of other forms of matter. Like the nucleus, a substance such as Silly Putty will deform into new shapes under a gentle collision, but will shatter like a piece of glass when subjected to a hard, rapid blow. There is evidence that the breakup of nuclei also sets in suddenly at energies of a few tens of MeV per colliding nucleon. The process may be used to measure the tensile strength of nuclear matter. It is suggested that the spallation debris of a nuclear collision could contain information about high density and shock waves in nuclei. The spallation reaction also plays an important role in determining the abundance of elements in the universe. In particular, ^{6}Li, ^{9}Be, ^{10}B, and ^{11}B are created from spallation of interstellar gas by galactic cosmic rays, which leads to collisions of hydrogen with abundant nuclei such as carbon, oxygen, and silicon. *See* ELEMENTS AND NUCLIDES, ORIGIN OF; NUCLEAR REACTION.

[DAVID K. SCOTT]

Bibliography: H. Reeves, W. A. Fowler, and F. Hoyle, Galactic cosmic ray origin of Li, Be and B in stars, *Nature*, 226:727–729, 1970; D. K. Scott, Towards relativistic heavy ion collisions, *Prog. Particle Nucl. Phys.*, 4:5–93, 1980.

Collision of an argon nucleus with a lead nucleus at an incident energy of 72,000 MeV in a streamer chamber. The nucleus is incident from the left. (*From L. S. Schroeder, Streamer chambers – their use for nuclear science experiments, Nucl. Instr. Meth., 162:395–404, 1979*)

Sparganosis

An infection by the plerocercoid, or sparganum, of certain species of the genus *Spirometra*. Members of this genus have a life cycle much like that of *Diphyllobothrium latum*. The adult normally occurs in the intestine of dogs and cats, the procercoid in copepods, and the plerocercoid in the musculature of frogs, snakes, or aquatic mammals, but not in fish. The whitish, unsegmented plerocercoid usually is an inch or so in length, but may reach a length of a foot or more. Man may become infected accidentally by drinking water with infected copepods or by eating hosts containing plerocercoids. Since humans are not suitable hosts for the adult stage, the plerocercoids leave the gut and enter the musculature, body cavities, or other sites and remain as plerocercoids. In the Orient, freshly opened frogs are sometimes used as poultices on sores, particularly around the eyes, and if plerocercoids are present, they may invade the human tissues. Human sparganosis is rare in North America. *See* PSEUDOPHYLLIDEA.

[REINO S. FREEMAN]

Spark chamber

A triggered electronic particle-detecting device whose purpose is to make visible and to locate accurately in space the tracks of charged particles. It is generally classified as wide-gap or narrow-gap; the most common form is a narrow-gap array of parallel-plate condensers, the plates of which are spaced about 3/8 in. apart, filled with a mixture of helium and neon at atmospheric pressure. A spark-chamber system requires an external initiating signal from an auxiliary particle-detection system, which triggers the application of a short-duration high-voltage pulse to the array of plates. The high-voltage pulse produces a spark discharge that

Nuclear Instruments and Methods 196 (1982) 33–40
North-Holland Publishing Company

BRAGG CURVE SPECTROSCOPY *

C.R. GRUHN, M. BINIMI, R. LEGRAIN, R. LOVEMAN, W. PANG, M. ROACH, D.K. SCOTT, A. SHOTTER, T.J. SYMONS, J. WOUTERS and M. ZISMAN
Nuclear Science Division, Lawrence Berkeley Laboratory, University of California, Berkeley, CA 94720, U.S.A.

R. DEVRIES, Y.C. PENG and W. SONDHEIM
Physics Division, Los Alamos National Laboratory, University of California, Berkeley, CA 94720, U.S.A.

A new method named "Bragg curve spectroscopy", based on the Bragg curve of the heavy ion being stopped in a gaseous ionization chamber, has been developed for identifying the particle and measuring its energy. The design of such a chamber and the experience obtained with the chamber using various kinds of fast heavy ions are described. In conclusion, several problems to be solved in this method are pointed out.

1. Introduction

We present in this paper an alternative way of using a gaseous ionization chamber in the detection of energetic heavy ions, which we call Bragg curve spectrscopy (BCS). Conceptually BCS involves using the maximum data available from the Bragg curve of the stopping heavy ion for purposes of identifying the particle and measuring its energy. A detector has been designed that measures the Bragg curve with high precision. From the Bragg curve we determine the range from the length of the track, the total energy from the integral of the specific ionization over the track, the dE/dx from the specific ionization at the beginning of the track, and the Bragg peak from the maximum of the specific ionization of the heavy ion. This last signal measures the atomic number, Z, of the heavy ion unambiguously.

Several advantages are realized in this type of heavy ion detector. The detector is relatively insensitive to radiation effects. Large solid angles are easily achieved. The resolution for identifying particles is intrinsically high because all the measurements are made in one medium eliminating window or dead layer effects. Particle identification can in principle be achieved over a large dynamic range of energies and particles.

This paper presents some of our initial experience with the BCS concept. We shall not compare this detector with alternative concepts. We shall emphasize the interpretation of our results and point out some of the remaining problems to be explored.

* Supported by USDOE.

0029-554X/82/0000-0000/$02.75

2. Detector design

The detector design is an ionization chamber with a Frisch grid to cathode distance longer than the range of the particles to be stopped. The anode to grid spacing is shorter than the lowest range heavy ion of interest. The particles enter through the cathode and leave an ionization track parallel to the electric field. The electrons along the track drift through the grid and are viewed as an anode current. The anode current as a function of time is proportional to the specific ionization along the track. The more important parameters of the detector used in this paper are presented in table 1.

We have used conventional NIM electronics to realize the results presented in this paper. The anode signal is viewed with a charge sensitive preamplifier. The preamplifier output is connected in parallel to the electronics which yields the energy, the Bragg peak, the range, and dE/dx of the particle. The energy signal is obtained using a shaping amplifier with a time constant

Table 1
Design parameters for BCS detector

Cathode to grid distance	28 cm
Grid to anode distance	3 cm
Grid wire diameter	40 m
Grid wire spacing	560 m
Electric field ratio (grid to anode/grid to cathode)	2.5
Cathode window	aluminized hostaphan
Voltage divider pitch	2 cm^{-1}
Gas	93% Ar+7% CH_4

PHYSICS REPORTS (Review Section of Physics Letters) 83, No. 4 (1982) 281–380. North-Holland Publishing Company

PIONIC MODES OF EXCITATION IN NUCLEI†

E. OSET‡

Department of Atomic and Nuclear Physics, University of Salamanca, Spain

H. TOKI

Cyclotron Laboratory, Dept. of Physics, Michigan State University, East Lansing, Michigan 48824, USA

and

W. WEISE

Institute of Theoretical Physics, University of Regensburg, D-8400 Regensburg, West Germany

Received September 1981

Contents:

† Work supported in part by German Bundesministerium für Forschung und Technologie (grant no. MEP 3200 X) and by Deutsche Forschungsgemeinschaft (grant no. We 655/7-4).

‡ Supported in part by Fundacion March.

Theories of Heavy-Ion Collisions.

G. BERTSCH (*)

Michigan State University - East Lansing, Mich. 48824

(Chapter from Nuclear Structure and Heavy-Ion Collisions, published in 1981 by North-Holland Publishing Co.)

(*) This work is supported by the National Science Foundation Grant PHY-7620097.

INSTITUTE OF PHYSICS

CONFERENCE PROCEEDINGS

NUCLEAR STRUCTURE
AND
PARTICLE PHYSICS

University of Oxford
6 – 8 April 1981

CRITIQUE OF NUCLEAR SPECTROSCOPY

B.H. Wildenthal

Cyclotron Laboratory, Michigan State University
East Lansing, Michigan 48824

1. INTRODUCTION

In using the term "Nuclear Spectroscopy" in this review I refer to that domain of nuclear physics which is concerned with the properties of the low-energy configurations of atomic nuclei. Typically, in a nucleus of given mass number A and charge number Z our attention is concentrated upon levels in the lowest ∿5 to ∿15 MeV of excitation energy or, equivalently, to collections of the lowest 5 to 10 energy levels of each different combination of total angular momentum J, parity π and isospin T.

The vitality of nuclear spectroscopy stems in large part from the capability of present experimental techniques to provide us with precise measurements of an amazing variety of different physical characteristics of these nuclear energy levels. Beyond quantum number assignments, properties which are unique to a single individual level can be determined only for ground states and an occasional excited state. But, for these states, the entire range of allowed multipole moments can be measured, together with the occupation probabilities for the quantum states of the constituent nucleons. Beyond these data for single states most measurements of nuclear spectroscopy concern the relationships between pairs of states. Techniques for determining these "relational" properties involve either "nucleon-transfer" processes, in which one or more nucleons are added to, or subtracted from, a target ("ground") state to form the various states of a residual nucleus, or "rearrangement" processes, in which there is a transition from one state to another of the same A-value.

Experimental information on nucleon-transfer properties, in the form of reduced matrix elements for the creation or annihilation of one or more nucleons in a specified cluster, is extracted from the analysis of the cross sections of nuclear reactions such as (p,d), (d,^{6}Li), (t,p) etc., with the appropriate theory for the reaction process. Information on rearrangement properties is obtained from weak-decay and electromagnetic-decay rates and electromagnetic and hadronic inelastic scattering reaction cross sections. Reduced matrix elements are easily extracted by classical formulae from measured decay rates. Analysis of inelastic scattering data to extract reduced matrix elements requires more complex tools.

I have schematically illustrated in Figs. 1 and 2 the information which current experimental nuclear spectroscopy can provide about a typical nucleus, here taken to be ^{23}Na. The essential message of this illustration is that a given nuclear state can be characterized in terms of a large number of different measurements. These measurements connect a given state to many other states of the same A, by a variety of physical processes, as well as to states of different A values. It is the task of theoretical nuclear spectroscopy to address the richness and density of these experimental data. However, existing theory treats these data from a variety of philosophical attitudes. One attitude I would characterize as being constrained by the desire to utilize simple and physically intuitive models to explain the data. The paradigm of such theories is the model of the nucleus as a rotating spheroid (ref. 1). Another attitude I would characterize as constrained by the desire to utilize elegant and/or concise formalisms in explaining data. Examples of such theories are the SU(3) model for light nuclei (ref. 2) and the I.B.A. (interacting boson approximation) for heavy nuclei (ref. 3).

DYNAMICS OF HEAVY-ION COLLISIONS
N. Cindro, R.A. Ricci and W. Greiner (editors)

LIGHT PARTICLE EMISSION IN HEAVY-ION COLLISIONS

David K. SCOTT

National Superconducting Laboratory
and
Departments of Physics and Chemistry
Michigan State University
East Lansing, Michigan 48824, USA

Abstract: Some aspects of light particle emission in heavy-ion collisions are discussed over a broad energy region from about 10 MeV/nucleon up to relativistic energies of 1 GeV/nucleon. The appearance of high energy components above the equilibrium evaporation region of the spectra is shown to be a general feature. At all energies the contributions to this tail are likely to range from single nucleon-nucleon up to multiple nucleon collisions. Various theories have been developed to describe the processes, ranging from the microscopic models of DWBA, master equation, cascade and TDHF to the macroscopic hydrodynamic, participant-spectator and hot-spot reaction mechanisms. A common feature of the macroscopic models is the formation of a localised participant zone in thermal equilibrium at high temperature. Systematics on the existence of this zone are presented over a wide range of energies, but other explanations in terms of simpler direct processes cannot be ruled out at this stage. The relation to short mean free paths and the contrast with low temperature mean field theories which ignore nucleon-nucleon collisions are mentioned. Various approaches to determining the size of the localised zones are presented, such as the geometry of the participant and hot-spot models, the formation of composite light particles by coalescence or by chemical equilibrium, and experiments on two particle intensity interferometry. Studies of the light particles, in particular the deuteron-proton ratio, to determine the entropy of the hot zone are also described. Although the observed excess at high energies is presently attributed to the influence of additional degrees of freedom, eg. from phase transitions, a note of caution is raised by similar studies at lower energies. It is possible that deuterons are also created by simpler mechanisms, eg. by the snowball and surface pick-up effects. Finally it is shown that the multiplicity of light particles, by probing the disintegration of the hot zone, can also give information on the equation of state of nuclear matter.

1. Introduction

The emission of light particles is now a frequently studied aspect of nuclear collisions, not only because light particles are often the most probable outcome of the reaction but also because they are a copious source of information about the mechanisms. In concert with the huge amount of experimental data amassed at incident energies from a few MeV/nucleon to relativisitic energies of several GeV/nucleon, there exists a plethora of theoretical interpretations, ranging from microscopic approaches of TDHF, pre-equilibrium and cascade models to the more macroscopic theories of nuclear hydrodynamics, hot spots, and participant-spectator models. In addition to supplementing the knowledge derived from light-ion reactions on the evolution of nuclear systems towards global or partial equilibrium, the light particles produced in heavy-ion collisions may also serve as harbingers of the conditions prevailing in the hot, dense matter presumed to be created at relativistic energies. In this paper we discuss recent results on light particle emission, emphasizing the insight to be gained by systematic studies over a wide energy region.

Nuclear Theory 1981

Proceedings of the
Nuclear Theory
Summer Workshop
Santa Barbara
August 1981

Edited by George F Bertsch

World Scientific Singapore
1982

IEEE Transactions on Nuclear Science, Vol. NS-28, No. 3, June 1981

CALCULATION OF FORCES ON THE ALUMINUM HEAT SHIELD PRODUCED BY EDDY CURRENTS DURING DISCHARGE OF A SUPERCONDUCTING CYCLOTRON MAGNET*

Felix Marti and M.M. Gordon
Cyclotron Laboratory, Michigan State University
East Lansing, MI 48824

Summary

The superconducting magnet in our 500 MeV cyclotron contains a (liquid nitrogen cooled) aluminum heat shield within the cryostat, and when, after more than two years of operation, the cryostat was disassembled, it was discovered that the outer surface of the heat shield had collapsed inward, thereby compressing the underlying super-insulation tightly against the can containing the liquid helium and coil. Consideration of the resultant geometry of the heat shield indicated that the collapsing force was produced by eddy currents generated in the aluminum either during discharge of the magnet or else when one of the radial support links happened to break. These forces have been calculated under both conditions, and the procedures used for these calculations are presented here together with the results. We conclude that the collapse of the heat shield was most probably caused when, on one occasion, the dump resistor accidentally burned out thereby producing an exceptionally fast discharge of the magnet.

Introduction

After more than two years of operation, the cryostat of the superconducting magnet in our 500 MeV cyclotron was disassembled in early 1980. The coil can is kept in a helium bath at 4°K. It is loosely wrapped in several layers of aluminized mylar (superinsulation) and enclosed in an aluminum container. This container consists of two concentric circular cylinders of radii 28.6 and 38.8 inches, with top and bottom ring-shaped covers; the height of the cylinders is 48 inches (see Figure 1). The container is kept in contact with liquid nitrogen, and works as a heat shield to decrease the radiant flow of heat toward the coil can.

MSUX-80-507

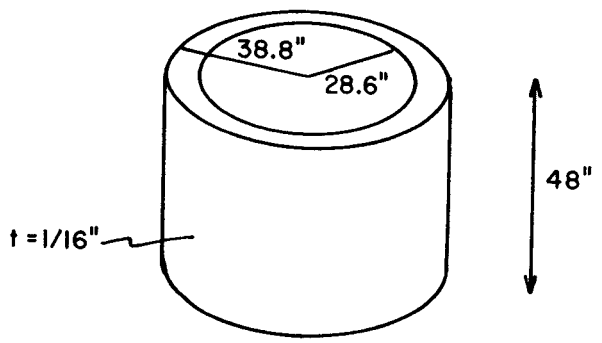

FIG. 1. Dimensions of the nitrogen cooled aluminum shield for the K500 superconducting coil.

After the cryostat was opened, it was observed that the exterior cylinder in the heat shield had collapsed toward the axis, resulting in the flattening of the outer lateral surface into an almost regular polygon, whose faces were tightly compressing the superinsulation against the helium can. This is an undesirable situation from the heat transmission point of view, reducing the path for conduction losses.

It was decided to study the different situations that could have produced the buckling of the outer cylinder. The inner cylinder did not show any sign of deformation.

Eddy currents are generated in the aluminum heat shield whenever the magnetic field changes. During a fast discharge of the magnet, the eddy currents interact with the strong axial field, applying a radial force that compresses the outer cylinder of the heat shield. The first possibility considered was that the buckling was caused by the eddy currents generated during a normal dump exercise. Second, the coil can is partially supported by three horizontal links, and in October 1977 one of these links broke, suddenly displacing the coil. This must have generated strong eddy currents similar to those produced during a dump. The third possibility analyzed was the accident which occurred in September 1977 when the dump resistor accidentally burned out and arcing was observed during what started as a normal dump.

Normal Dump

In case of an emergency, e.g., quench of one of the coils, the energy stored in the superconducting magnets is dumped into a 0.3Ω resistor submerged in water. The current in the magnet discharges then as

$$I(t) = I_o e^{-\lambda t} \quad , \text{ with } \lambda = \frac{1}{150}\ s^{-1} \tag{1}$$

The magnetic flux ϕ enclosed by any closed curve will decrease according to

$$\frac{d\phi}{dt} = -\lambda\phi \quad . \tag{2}$$

Considering a cross section perpendicular to the axis of the heat shield, and selecting an integration path C contained in the shield, we have, by Faraday's law,

$$\oint_C \vec{E}\cdot d\vec{\ell} = -\frac{d\phi}{dt} = -\frac{d}{dt}\int_S \vec{B}\cdot\vec{n}\ ds$$

$$= -\frac{d}{dt}\int_S \nabla x\vec{A}\cdot\vec{n}\ ds = -\frac{d}{dt}\oint_C \vec{A}\cdot d\vec{\ell} \tag{3}$$

where $\vec{E}$ is the electric field, $\vec{B}$ the magnetic field and $\vec{A}$ its vector potential. $\vec{n}$ is the unit vector normal to a surface S with boundary on the curve C. Given the axial symmetry that our system has, we can write:

$$E_\theta = -\frac{\partial A_\theta}{\partial t} = \lambda A_\theta \tag{4}$$

The force per unit volume is

$$\frac{dF}{dv} = \vec{J} \times \vec{B} \ , \tag{5}$$

where

$$\vec{J} = \sigma\vec{E} \ , \tag{6}$$

and σ is the conductivity of the aluminum sheet. The pressure on the lateral face is

$$P_L = \frac{dF}{dS} = \left|\vec{J} \times \vec{B}\right| t = \sigma E_\theta B_z t \tag{7}$$

0018-9499/81/0600-3254$00.75©1981 IEEE

WORKSHOP ON HIGH-RESOLUTION, LARGE-ACCEPTANCE SPECTROMETERS
Argonne National Laboratory, Argonne, IL, September 8-11, 1981

Why use superconducting coils in conventional spectrograph magnets?

J.A. Nolen, Jr.
National Superconducting Cyclotron Lab
Michigan State University
East Lansing, MI 48824

ABSTRACT

This report presents an analysis of the costs of large spectrograph dipoles with conventional copper coils compared with ones utilizing superconducting coils. For large gap magnets (~ 15 cm), the superconducting version is significantly less expensive to build as well as to operate. The copper-coil dipole would also be about 50% more massive than the superconducting version.

Supported in part by the NSF Grant # PHY 80-17605 and
DOE Grant # DEAC-02-80ER-10579

WORKSHOP ON HIGH-RESOLUTION, LARGE-ACCEPTANCE SPECTROMETERS
Argonne National Laboratory, Argonne, IL, September 8-11, 1981

Modifications to POISSON

L.H. Harwood
Cyclotron Laboratory, East Lansing, MI 48824

At MSU we have used the POISSON(1) family of programs extensively for magnetic field calculations. In our presently super-saturated computer situation, reducing the run time for the program is imperative. Thus, I have made a series of modifications to POISSON to speed up convergence. Two of the modifications aim at having the "first guess" solution as close as possible to the final solution. The other two aim at increasing the convergence rate. In this discussion, a working knowledge of POISSON is assumed. The amount of new code and expected time saving for each modification is discussed.

The first modification is quite simple. POISSON allows the result of a previous calculation to be used as the start for a subsequent case if the latter differs from the former by only an overall scaling of the current densities involved. This is accomplished with a scaling factor XJFACT. The full potential of this feature is not utilized by POISSON. By adding a single line of code, a time savings of 5-90% can be achieved. Quite simply, originally when the program changed the current densities, it did not scale the vector potential array. In an infinite permeability or an iron-free case, the vector potenial scales linearly with current density. If this scaling is included then the overrelaxation needs only to account for saturation effects. At very low or very

WORKSHOP ON HIGH-RESOLUTION, LARGE-ACCEPTANCE SPECTROMETERS
Argonne National Laboratory, Argonne, IL, September 8-11, 1981

Superconducting "Panofsky" Quadrupoles

Leigh H. Harwood

Cyclotron Laboratory,

East Lansing, MI 48824

A design for a rectangular aperture quadrupole magnet without pole-tips was introduced by Hand and Panofsky in 1959 (1). This design was quite radical but simple to construct. Few magnets of this design were ever built because of the large power needed. With the advent of superconducting coils there has been a renewed interest in them. The mathematical basis, field characteristics, and present and future construction of these magnets will be described below.

Mathematical basis: The P.Q. design is shown in fig 1. That a perfect quadrupole field can be produced with so simple a design is initially quite surprising. However, the P.Q. is a member of a family of magnet designs called "current sheet magnets" by Ikegami[2]. These magnets are based on a cavity in a shell of infinite permeability iron which is lined with an infinitesimal current sheet. If ϕ is the magnetostatic potential for the problem and j is the linear current density, then (2) $j = -\frac{\partial \phi}{\partial s}$ where $\frac{\partial \phi}{\partial s}$ is the derivative of the potential tangent to the surface. For a 2N-pole field, $\phi = A_{2N} r^N \sin(N\theta)$. Thus, $j = -NA_{2N} r^{N-1} \sin(\alpha + (N-1)\theta)$ where α is the angle between the tangent to the surface and the x-axis.

Consider a rectangular shell. If we substitute N=2 (quadrupole) and $\alpha = \frac{\pi}{2}$ (a vertical surface), we get $j = NA_{2N} r \cos(\theta) = \beta x$ where β is a constant. For this

WORKSHOP ON HIGH-RESOLUTION, LARGE-ACCEPTANCE SPECTROMETERS
Argonne National Laboratory, Argonne, IL, September 8-11, 1981

Dipole Design Studies for the MSU 1.2 GeV/c Superconducting Spectrograph*

A.F. Zeller, J.A. Nolen, Jr., and L.H. Harwood

Cyclotron Laboratory

Michigan State University

East Lansing, MI 48824

ABSTRACT

This report summarizes the results of a series of calculations for a large gap (6") "window-frame" dipole with superconducting coils. These studies led to a design which has a large region of good field, low mass, and large dynamic range [5-16 kG]. It's disadvantage is relatively complicated superconducting saddle coils.

* Research supported by NSF PHY 80-17605 and

DOE DEAC-02-80-ER-10579

WORKSHOP ON HIGH-RESOLUTION, LARGE-ACCEPTANCE SPECTROMETERS
Argonne National Laboratory, Argonne, IL, September 8-11, 1981

Phase Space Rotation with Solenoids and Quadrupoles*

J.A. Nolen, Jr.

National Superconducting Cyclotron Laboratory

Michigan State University

East Lansing, MI 48824

ABSTRACT

In this report a standard five-quadrupole phase-space rotation system is discussed and compared with a possible alternative - two superconducting solenoids which accomplish the same job in a different way. In some laboratories the solenoid system may be advantageous.

*Supported by the National Science Foundation-Grant No. PHY 78-22696 and Department of Energy Grant No. DOE-DEAC-02-80-ER-10579.

WORKSHOP ON HIGH-RESOLUTION, LARGE-ACCEPTANCE SPECTROMETERS
Argonne National Laboratory, Argonne, IL, September 8-11, 1981

Optimizing Energy Resolution in Accelerator-Spectrograph Systems*

E. Kashy

National Superconducting Cyclotron Laboratory
Michigan State University
East Lansing, MI 48824

This paper describes the optimization of energy resolution in magnetic spectrograph systems and at the same time compares two significantly different systems, the HHH and VHV systems. In the first, HHH, we have in the same plane, the incident beam dispersion, the nuclear reaction or scattering, and the spectrograph analysis, the plane being commonly the Horizontal plane. In the second scheme, VHV, which is the case for the Los Alamos HRS[1] (High Resolution Spectrograph), the incident beam dispersion and the analysis of the reaction products by the spectrograph are in one plane (vertical), while the reaction plane is an orthogonal plane, (horizontal). This latter scheme, VHV, has been selected for the high resolution 1.2 GeV/c spectrograph[2] to be used in the study of heavy-ion reactions at the National Superconducting Cyclotron Laboratory (NSCL) which is being constructed on the campus of Michigan State University.

We begin by referring to some empirical methods for tuning the accelerator-beam transport-spectrograph system.

*This material is based upon work supported by the National Science Foundation under Grant No. Phy 80-17605.

WORKSHOP ON HIGH-RESOLUTION, LARGE-ACCEPTANCE SPECTROMETERS
Argonne National Laboratory, Argonne, IL, September 8-11, 1981

Optimization of Induced Aberrations in Ion Optical Systems

L. H. Harwood, J. A. Nolen, Jr., and K. L. Brown*
Cyclotron Laboratory, Michigan State University,
East Lansing, MI 48824

Abstract

The problem of designing an ion optical system with the minimum line width is addressed in this paper. The importance of the effects of the details of the first-order layout on the higher order aberrations is discussed. Procedures for minimizing the induced third and higher order aberrations are presented. We also present a technique for testing if these higher order aberrations are important when only second order intrinsic aberration matrices are available.

WORKSHOP ON HIGH-RESOLUTION, LARGE-ACCEPTANCE SPECTROMETERS
Argonne National Laboratory, Argonne, IL, September 8-11, 1981

Integrated Magnet, Optics and Detector Designs for a Spectrograph*

J.A. Nolen, Jr.
National Superconducting Cyclotron Laboratory
Michigan State University
East Lansing, Michigan 48824

ABSTRACT

This report illustrates how the physics measurement goals, practical considerations and/or restraints, beam properties, and detector limitations can all be integrated to lead to an optimized spectrograph design. The various measurement goals are considered iteratively or interactively with the magnetic and detector limitations and specifications to achieve a cost effective design with an enhanced probability of success.

*This material is based upon work supported by the National Science Foundation under Grant No. PHY-22696 and DOE-DEAC-02-80-ER 10579.

WORKSHOP ON HIGH-RESOLUTION, LARGE-ACCEPTANCE SPECTROMETERS
Argonne National Laboratory, Argonne, IL, September 8-11, 1981

The MSU 1.6 GeV/c Beam Analysis System*

J.A. Nolen, Jr.

National Superconducting Cyclotron Laboratory

Michigan State University

East Lansing, MI 48824

ABSTRACT

This report describes the design of the beam analysis system which is to prepare the beam for the large high-resolution spectrograph to be used with the superconducting heavy ion cyclotrons at MSU. The system has a momentum resolving power of over 20,000 with a 1 mm object slit and is of a very flexible, modular design which is readily adaptable to other applications.

*This material is based upon work supported by the National Science Foundation under Grant #NSF78-22696 and DOE-02-80-ER-10579.

WORKSHOP ON HIGH-RESOLUTION, LARGE-ACCEPTANCE SPECTROMETERS
Argonne National Laboratory, Argonne, IL, September 8-11, 1981

The MSU 1.2 GeV/c Spectrograph*

A.F. Zeller, J. Nolen, L.H. Harwood and E. Kashy

National Superconducting Cyclotron Laboratory

Michigan State University

East Lansing, MI 48824

The philosophy and principles outlined in previous papers (see other conference contributions from these authors) were the basis on which the 1.2 GeV/c spectrograph was designed. The basic layout of the MSU spectrograph is shown in figure 1, complete with the beam analysis system. Figure 2 shows an enlarged side view of the spectrograph. Figures 3-6 are engineering sketches of the pit and support structure needed to convert the magnets into a working spectrograph.

Design goals and physical parameters for the system are listed in Table 1. It should be noted that the final magnet weights are not completely determined since we are still investigating alternatives to the somewhat complex saddle coil approach. The total costs (1981$) will be approximately $1.7 million, including the beam analysis system.

*Research supported by the NSF, Grant No. PHY 80-17605 and

DOE #DEAC-02-80-EI-10579

DESIGN CALCULATIONS FOR THE CENTRAL REGION OF THE NSCL 500 MEV SUPERCONDUCTING CYCLOTRON*

F. Marti, M.M. Gordon, M.B. Chen,[a] C. Salgado, T. Antaya and E. Liukkonen[b]

Cyclotron Laboratory, Michigan State University, East Lansing, MI 48824 USA

Abstract.-The 500 MeV superconducting cyclotron has three 60° dees within the magnet valleys, and the design of the central region is complicated because it must accommodate the inner tips of these dees, the tips of the three intervening dummy dees, and the ion source, all within a very small space. In addition, this cyclotron is designed to operate on harmonics from h=1 to 7, with dee voltages up to 100 kV, and must accelerate a wide variety of heavy ions with turn numbers from n=100 to 600. To satisfy these diverse requirements, the overall plan for the central region calls for the construction and use of many different, but readily interchangeable sets of electrode structures with each set designed for a different range of operating conditions.

The procedure for determining the optimum geometry for a set of electrodes involves a converging sequence of tentative designs each of which is tested and improved through a combination of electrolytic tank measurements and orbit computations. For this purpose, the speed and accuracy of the tank measurements have been improved, and the resultant potentials are used in our computer programs to determine whether the ion orbits clear the obstacles successfully, gain energy efficiently, receive adequate vertical focusing, and finally emerge from the central region properly centered. The vertical motion computations are by far the most difficult, and a special effort has been made to obtain satisfactory results.

The 3D-Cyclone orbit program is an important tool for the design of the electrode structures in the central region of the 500 MeV superconducting cyclotron.[1] This program is a revised and enlarged version of the Cyclone code used in the design of our old 50 MeV cyclotron.[2] In addition to computing orbits in the electric field of a three dee rf system, the new program can also calculate the linear z motion in these fields.

The 3D-Cyclone program actually consists of three separate orbit codes which have been woven together so as to make possible the tracking of ion orbits starting from the source slit and going all the way out to the middle of the machine. Part I takes the ion from the source slit out to just beyond the puller. Part II continues the orbit for a few turns until it reaches r=2.8 in. Part III then takes the orbit as far as desired. These three parts differ mainly in the way they treat the rf electric field.

All three parts use the same median plane magnetic field $B(r,\theta)$ which is stored in a polar mesh with $\Delta\theta$=1.0 deg, and Δr=0.5 in. All such fields are produced by a separate set of special programs which tailor these fields to satisfy specific focusing and isochronism requirements. The magnetic field provides an absolute reference frame for positioning all of the electrodes and the resultant electric field used in the 3D-cyclone program.

For a given electrode geometry, an electrolytic tank is used to measure the median plane potentials $U(x,y)$ in a square mesh measuring 5.6 in on a side and with a uniform spacing $\Delta x = \Delta y$ = 40 mils. Each potential map thus contains 140 x 140 points and, because of recent improvements, now requires only 4 hours to measure. The accuracy and smoothness of the data have been tested using the geometry shown in fig. 1, and seem satisfactory for our purposes.

In Part I, the electric field in the source-puller region is derived from the potential: $V(x,y,t) = U_o(x,y)\sin\omega_{rf}t$, where $U_o(x,y)$ is mapped using an enlarged scale model of the electrode structures, and a sample map is shown in fig. 2. Such potential maps are

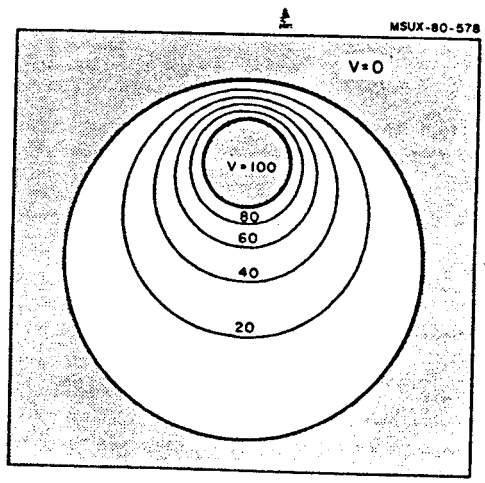

Fig. 1: Electrolytic tank test set-up. To check the accuracy of the electrolytic tank facility, we measured the potential between two cylinders. This is a two dimensional geometry where one of the cylinders is inside the other, but not coaxial with it. The theoretical potential distribution is given by a fairly simple analytic expression. The discrepancies between measurement and theory are within one percent of the potential difference applied between electrodes. This figure shows the equipotentials derived from such a measurement. The largest deviations occur when the probe is very close to the electrodes.

available for several different source-puller geometries, since each geometry will be fixed in the machine except for a possible rotation of the ion source by ±5 deg about its axis. The orbit computations in this part of the program are carried out in cartesian coordinates with t as the independent variable, and do not include z motion.

The electric field for Part II of the program is more complicated. The three dees with the three intervenining dummy dees, along with the ion source, all

STATUS REPORT ON THE 500 MEV CYCLOTRON *

Peter S. Miller and MSU Staff

Cyclotron Laboratory, Michigan State University, East Lansing, MI 48824, USA

Abstract.-The status of the K500 cyclotron construction is reviewed as of August 1981. The first operating tests are anticipated in two months.

1. Introduction.-The assembly of the K500 cyclotron will soon be carried far enough to allow testing with internal beam. The accompanying figures illustrate the progress that is being made.

2. Discussion.The conceptual design of the cyclotron systems is unchanged from that reviewed in the 1978 Conference, but many details have been modified as guided by prototype testing.[1] An example is the rf resonator which was assembled in a test vacuum chamber with a simulated dee electrode and was run at full power to verify the capability for maintaining 100 kV for extended periods. To achieve this it was necessary to modify the sliding shorts so that the contacts are positively clamped when rf is applied.

The 3 rf transmitters are at present under test using 50 kW water loads to simulate the resonators which are being assembled on the magnet.

The copper liners for both poles are installed and are vacuum tight. The coaxial resonators are being installed and leak-checked. The completion of the beam vacuum chamber, i.e. assembly of cryostat, liners and resonators on the magnet is expected by early September. The cryolines for the cryopumps in the dees are installed in the dee stems.

The superconducting coil was removed from its cryostat in early 1980 in order to install the median plane penetrations through the coil bobbin and the cryostat. These penetrations serve the electrostatic deflectors, the magnetic channels, the beam probe and the beam extraction path. The aluminum radiation shield was replaced with one of new design which has improved nitrogen cooling to the upper portions reduces the temperature there to about 80 K as desired. The total heat leak to the coil is close to what it was before these modifications were done.

The inner wall of the cryostat, made of mild steel except near the median plane, is the cyclotron vacuum wall. It was nickel-plated to prevent rust and to reduce the gas load on the pumps.

The magnetic field was mapped in 1980 to determine the details of the iron-produced field. The focusing and phase characteristics of a number of representative ions were calculated, and several iron shims were designed to optimize the performance of the cyclotron. These calculations took note of the expected effect of drilling 156 holes for trim coil leads and 18 others for rf and vacuum components. After these holes were drilled, the trim coils and the magnetic extraction elements were installed and the field mapping was repeated with the final iron configurations. The results agree with the calculations mentioned above.

The power supplies for the main magnet coils are being modified to increase the long-term stability of the currents and to make them compatible with the computer control system. The control system for the cyclotron is CAMAC - based and employs a low speed auto-polling network designed and built at MSU to lower costs by creating a buss for each CAMAC slot to increase the number of devices served. The controls and readings from all components in the cyclotron and experimental equipment will be integrated in the system.

The operator controls the cyclotron through two linked computers using a combination of fixed function and multiplexed knobs, switches and displays. The values of interest to the operator are read by the computers and displayed on meters, digital registers, lights or on a television monitor. The system is presently operating with the beam probe, trim coils and harmonic coils connected to it.

*This material is supported by the NSF under Grant No. PHY 80-17605.

References

1. H.G. Blosser, IEEE Trans. on Nucl. Sci. NS-26, No. 2 (1979) 2040.

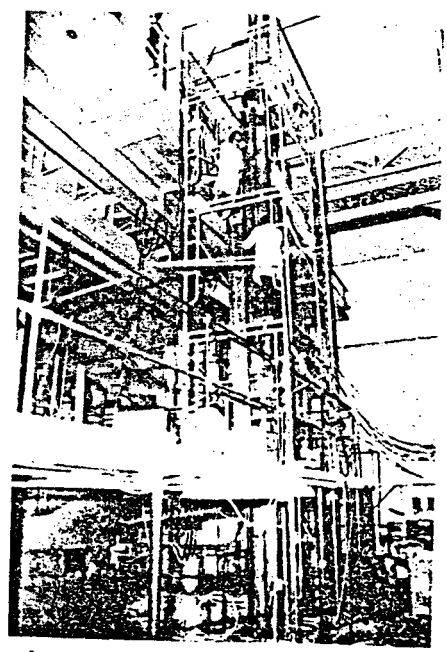

Fig.1: View of the rf test resonator. Most of the upper stem and part of the lower stem are visible. The dee is in a circular aluminum vacuum chamber partly visible through the railing near the center. One of the copper panels of the outer conductor is being installed by the workers.

STATUS REPORT ON THE 800 MEV CYCLOTRON*

M.L. Mallory and MSU Staff

National Superconducting Cyclotron Laboratory, Michigan State University, East Lansing, MI 48824, USA

Abstract.-The status of the K800 cyclotron project is reviewed as of August 1981.

1. Introduction.-The 800 MeV superconducting cyclotron has been in the construction phase since October 1979 and work on major components is well advanced. Eighteen sections of the magnet yoke have been cast and are in the process of machining. The wire conductor for the coil is now drawn and the operation of soldering the conductor to the substrate is completed and 80% of it is delivered. Welding of the coil bobbin is nearly complete and final machining operations are to begin shortly. The anode power supply for the rf system is under construction and approximately 50% assembled and the large central helium refrigerator is nearing final

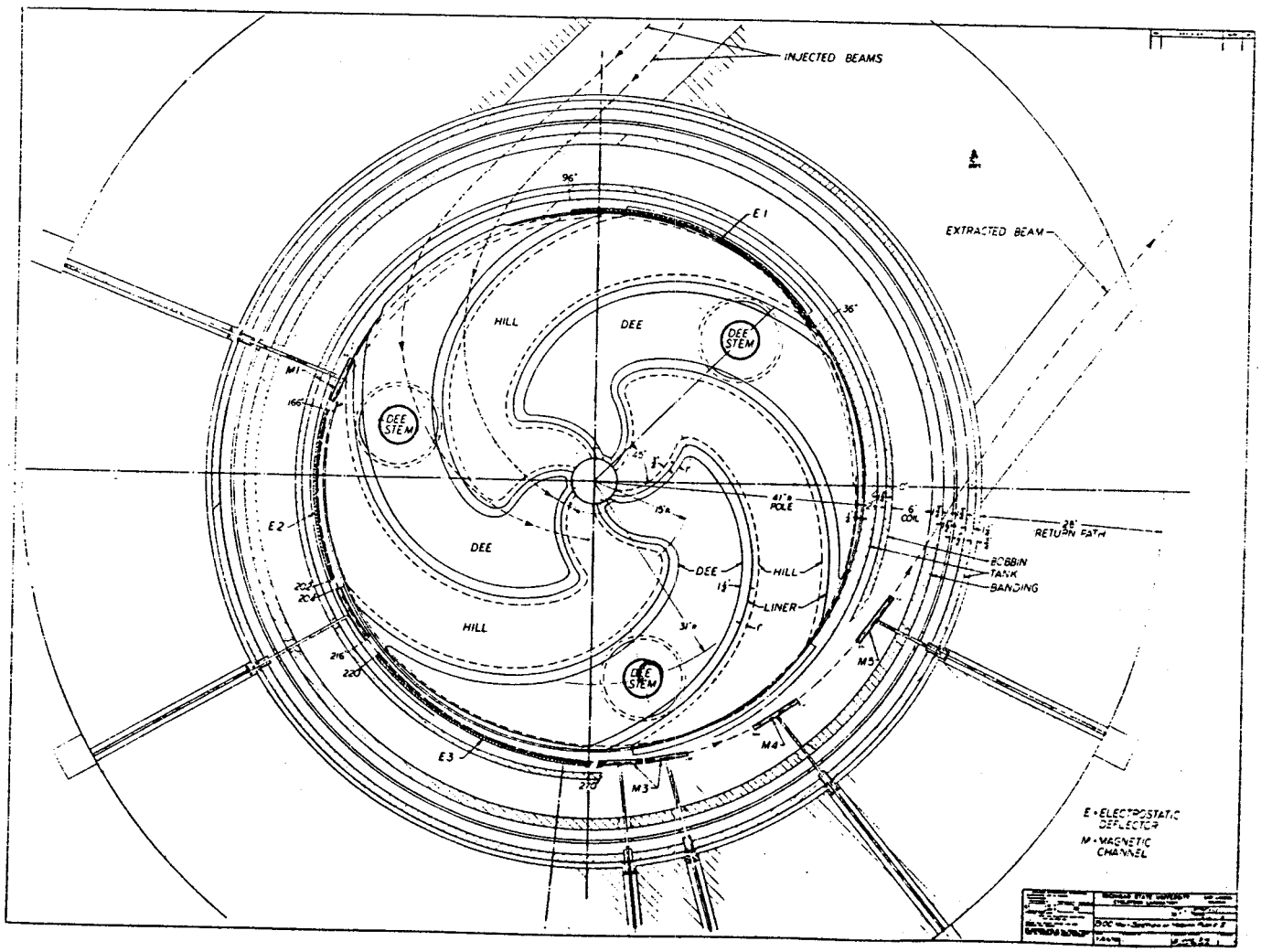

Fig. 1: A plan view of the cyclotron magnet is shown. The unique pole tip configuration was necessary to accommodate the various injected beam trajectories and allow stripping to a higher charge state outside the rf dee structure. The pole radius is 43.25" (including the cryostat inner wall).

THE MAGNETIC FIELD OF THE K500 CYCLOTRON AT MSU INCLUDING TRIM COILS AND EXTRACTION CHANNELS*

P. Miller, D. Johnson and H. Blosser

National Superconducting Cyclotron Laboratory, Michigan State University, East Lansing, MI 48824, USA

Abstract.-A field mapping program has been carried out in the K500 cyclotron with all magnetic components in place to obtain a data in computer files needed to find operating settings for any desired beam. The set of measurements includes the effect of pole tip shims installed after previous magnetic field measurements to compensate for holes drilled for rf and trim coil penetrations. These shims produce the desired field changes. A small hysteresis effect appears in the radial profile of the average field; it is eliminated by a simple turn-on cycle. Hysteresis effects from trim coil excitations are negligible, but the trim coil field intensity depends slightly on the central field level. Also, the trim coil field is measurably stronger than the air core calculation predicts. The first harmonic of the ν_r=1 resonance is controlled by varying the current distribution in the 3 sectors of trim coils 1 and 13. The magnetic extraction elements are passive iron focusing channels, designed in the saturated iron approximation. The first harmonic of the stray field is compensated at a radius near the extraction radius. The measurements verify in detail the accuracy of stray field calculations for the focusing bars.

1. Introduction.-The K500 magnet was dismantled in spring of 1980 to install trim coils and to make penetrations through the midplane sections of the coil and cryostat for extraction elements. The location of the magnetic channels (M_1-M_8) and the magnetic compensating bars (C_1 and C_2) are given in Fig. 1. Some iron shims were also added and removed to adjust the average field and the flutter according to calculations with previously measured field maps,[1,2] The design of these shims took note of the effect of drilling 156 holes for trim coil leads and 18 others for rf couplers, trimmers etc. These additional holes, shown in Fig. 2, were drilled in the poles while the magnet was apart. After these installations, the re-assembled magnet was field mapped again starting in January 1981. These maps are the data for predicting the main coil currents, trim coil currents and focusing bar positions needed for any beam. The mapping apparatus measured the field with an accuracy of approximately ±10 G. This figure is dominated by the estimated effect of slow unpredictable changes in the calibration constants for the flip coils which occured continuously.

2. Experiments and results.-The operating region of the cyclotron, between B_o=30 kG and B_o=49 kG (B_o= central magnetic induction) was covered with a grid of 15 points in the coordinate plane defined by the currents in the small and large main coils, called I_α and I_β respectively (see Fig. 3). The accuracy of interpolation in this size grid was verified experimentally. It was necessary to develop a standard turn-on cycle to avoid a small hysteresis effect in the radial profile (≤20 G). An example of this effect is shown in Fig. 4. A short circuit developed during operation at the highest excitation (I_α/I_β=600 A/800 A) which persisted thereafter but had no measurable effect on the steady state field of the magnet, although it constrained the current rampings to be slower than usual to limit the axial forces in the coil support links. Since the short circuit made it impractical to include maximum excitation in a turn-on cycle, the chosen cycle began at field 0 (see Fig. 3) and followed the solid line until the desired sum $I_\alpha+I_\beta$ was reached. Then one adjusted I_α and I_β to desired values, keeping the sum fixed.

The trim coils were mapped at 4 main excitations near the corners of the base field grid. Hysteresis effects from main coil or trim coil excitation on the trim coil - produced field were found to be negligible. The average field from each trim coil was slightly larger than the calculated field assuming air core coils and varied a few percent with excitation, presumably due to saturation of the yoke. Figure 5 shows an example of the experimental and air-core average fields.

As a check of the iron field and to verify trim coil superposition, the field was mapped with all trim coils turned on at the calculated settings for E/A = 80 MeV/u, Q/A = .5, e.g. deuterons. When the phase and focusing behavior of the particle were calculated in the measured field the results were as expected.

The shape of the edge field (R>26.5 inches) was inferred from measurements at 5 azimuths where holes exist in the median plane so the field measuring probe could be displaced radially into the coil. The field modulation was taken into account, and the average field in the region 27 in.≤R≤40 in. was obtained for each of the base fields. This allows the total field to be calculated at any azimuth along the trajectory of the extracted beam out to R=40 in. to an estimated accuracy of ±50 G.

3. Discussion.-The passive magnetic channels were designed using surface current (saturated iron) calculations of the field perturbations that they produce.[3] These calculations were verified experimentally in two ways:

SUPERCONDUCTING CYCLOTRON MAGNET COIL SHORT*

M.L. Mallory, H.G. Blosser, D.J. Clark, H. Laumer, D. Lawton, P. Miller and F. Resmini

National Superconducting Cyclotron Laboratory, Michigan State University, East Lansing, MI 48824, USA

Abstract.-In February 1981, a short circuit appeared in the superconducting coil of the K500 cyclotron. The short is resistive in character and therefore has no effect on steady state operation of the magnet. The resistance of the short varies, sometimes being below the threshold of detection as a heat load on the cooling system and sometimes being significant. The resistance under certain conditions shows approximately cyclic phenomena with time constants in the range of seconds and other approximately cyclic phenomena which correlate with gross operating parameters of the magnet (shifting current from one coil to another at high field and lowering and raising the liquid helium level). A number of diagnostic studies of the short have been made, using 1) an array of flux sensing loops to sense the magnetic effect of the short, 2) voltage comparisons between upper and lower sections of the coil, 3) comparisons of forces in the nine member coil support system and 4) the effect of the short on the thermal characteristics of the coil. Insulation failure or a metal chip shorting out turns have been explored in some detail but a convincing determination of the exact cause of the short may never be available, (even the extreme step of unwinding the coil having a significant probability that an imperfection with the observed characteristics would pass unnoticed). Analysis of the characteristics of the short indicated that the most serious consequence would be failure of the coils mechanical support system in the event that the magnet was quickly discharged, as in a dump or quench. To deal with this hazard, the support system has been modified by installing solid supports which prevent the coil from moving by an amount sufficient to damage the support system. We have also reexamined the data and calculations used in he original coil design and have made some additional measurements of the properties of the materials (yield strength, friction coefficient, Young's modulus) used in the coil construction.

1. Introduction.-In the winter of 1980-81, the final magnetic field measurements of the K500 cyclotron were being completed. A prescribed operating procedure, running the magnet to full excitation and then to a measuring point to minimize magnetic hysteresis effects,[1] was being executed when an imbalance between the voltage within the coil was detected and at the same time an anomalously high helium boiloff rate was observed. A diagnostic program was immediately initiated and in the following sections we describe the results so far obtained.

2. Detection of coil short.-Figures 1 and 2 are simplified drawings of the coil physical layout and the electrical circuit diagram.[2] The most enlightening data have been obtained with two magnetic flux pickup single turn wire loops ("$\dot{B}$ coils") located between the small and large coil, above and below the magnet symmetry plane (see Fig. 1). Additional measurements have been made with multiple B coils placed external to the coil vacuum jacket and two solenoids mounted around the top and bottom coil sets. The data gathered with these detection devices are presently unclear because of limited use. Figure 3 shows a transient B event. The cyclotron magnetic field at 4T is decreasing at a constant rate. The upper and lower B coils detected changes of opposite polarity in the magnetic flux. Figure 4 shows an intentional short, connected through 36Ω, across the voltage tap of the small coil and carrying 0.2 amps (~200 ampturns), (see Fig. 2) while the magnet is being charged, which closely reproduces the observed transient event of Fig. 3. (An ambiguity exists in that the large coil might recouple the $\dot{B}$ coils in the opposite sense from the small coils in which case the signal would indicate that the short is in the bottom large coil.)

A hard short, the condition of a continuous short, could be produced in the coil by charging the magnet up to maximum field with 800 amperes in the small coil and 600 amperes in the large coil and then swapping current between the large and small coil. The swapping of current results in a small change in magnet field, but a large change in forces on conductors. An example of the $\dot{B}$ data for a hard short is shown in Fig. 5 and indicates large flux deviations of up to 10,000 ampere turns. Figure 6 is a $\dot{B}$ measurement made at the beginning of charging the magnet with a hard short present. The asymmetry in the $\dot{B}$ data is larger when charging the large coil and there is a time lag in the upper $\dot{B}$ loop relative to the lower; these data then support a "short-in-the-upper-large-coil" hypothesis.

3. Coil short force.-The coils are suspended by nine fiberglass links and the force on each link is monitored by strain gauges. In the hard short condition, the forces were detected and had an appearance of possible runaway when the magnet was charged or discharged at full voltage.

An axial force between coil and iron of course comes from the interaction of the current in the shorted superconducting loop with the radial component of the magnetic field in the iron. This is awkward to calculate since the dominant component of B_r is due to the coil itself and this component of course produces no net force on the total coil. A series of relaxation calculations were run with several gross assumptions for the distribution of ampere turns in the short, the coil field was subtracted, and the net force between coil and iron was then calculated by integrating the interaction

Particle Accelerators
1982 Vol.12 pp.13-26
0031-2460/82/1201-0013$06.50/0

RADIAL-LONGITUDINAL COUPLING IN CYCLOTRONS AND FOCUSING COMPLEMENTARITY*

M. M. GORDON and FELIX MARTI

Cyclotron Laboratory, Michigan State University, East Lansing, Michigan 48824 USA

(Received August 6, 1981; in final form October 21, 1981)

The coupling of radial and longitudinal motion in cyclotrons is reconsidered, and following Schulte and Hagedoorn, the definition of the phase ϕ is revised so as to make it a constant of the motion for a monoenergetic group of ions executing radial oscillations. This revision helps to preserve energy homogeneity for the group, and also provides a simpler evaluation of the inertial force acting on the radial oscillations as a result of the outward shift of the equilibrium orbit at each gap crossing. This force is shown to produce what might be called "radial electric focusing" since it strongly resembles, and is actually complementary to, the well-known vertical electric focusing. That is, acceleration conditions which increase the vertical focusing will simultaneously decrease the radial focusing to a comparable extent. The resultant change in ν_r is evaluated for a fairly general *dee* geometry, and the conditions for radial instability near $\nu_r = 1$ are then discussed. These results are applied to a variety of cyclotrons including one at Indiana and the TRIUMF machine. In the latter case, some detailed calculations are presented to demonstrate how well the simple theory works when the acceleration is strongly non-adiabatic, but the motion is still linear.

1. INTRODUCTION

For most cyclic accelerators, the fractional energy gain per turn is so small that the acceleration process can be accurately described as "adiabatic". The most common exceptions to this rule are cyclotrons with fixed frequency rf systems since these machines accelerate ions for relatively small numbers of turns starting, in most cases, from nearly zero energy.

As a result, the median plane motion in cyclotrons is accompanied by an unusually strong coupling between the acceleration process and the radial oscillations within the beam. The strength of this coupling varies inversely with turn number, so that its effects are most pronounced in the central region. In many cases, however, these effects remain significant throughout the cyclotron. This is especially true when the rf system operates on a high harmonic of the orbital frequency since the coupling strength is also proportional to the harmonic number.

Certain aspects of the coupling process have been known for a long time, but the analytical treatments have all been rather specialized. There is, for example, the effect of a voltage asymmetry in classical cyclotrons, which was analyzed by Cohen.[1] In addition, there are the "electric gap crossing resonance" phenomena associated with the use of one or two dees in cyclotrons with three sector magnets.[2]

More recently, Schulte and Hagedoorn[3] have undertaken the first serious attempt at a comprehensive analysis of all coupling and other effects associated with median plane motion in cyclotrons. Unfortunately, their analysis is based on a nonrelativistic Hamiltonian and formulated in Cartesian coordinates, and both of these premises impose rather severe restrictions on the scope and accuracy of their results.

Nevertheless, their impressive work has clearly outlined at least two important aspects of the coupling process which deserve further exploration. One of these concerns the proper definition of the phase ϕ for particles executing radial oscillations about an equilibrium orbit. The second, related effect concerns a phase dependent shift in ν_r produced by the acceleration process which can, in certain cases, lead to radial instability.

Regarding the phase definition, one has, on the one hand, the phase ϕ which determines the energy gained by a group of particles when averaged over many gap crossings and, on the other hand, the "local" phase $(\omega_{rf}t)$ which specifies the time at which different members of the group cross a particular gap. The problem of correlating these phases was solved, at least for a nearly

* Work supported by the National Science Foundation under Grant No. Phy 78-22696

Contribution to the Proceedings of the Relativistic Heavy Ion Winter School, Banff, Alberta, Canada

ENERGY DEPENDENCE OF THE DISASEMBLY OF NUCLEAR MATTER

Gary D. Westfall
National Superconducting Cyclotron Laboratory
Michigan State University
E. Lansing, MI 48824

An important concept in high energy nucleus-nucleus collisions concerns the formation of a highly excited, localized region of participant nucleons moving with a velocity in the laboratory frame intermediate between the target and projectile velocities. The study of this zone as a function of incident projectile energy can provide information about the behavior of nuclear matter at densities and excitations far from the normal ground state.

In Figure 1, different modes for the interaction of two high energy nuclei are shown. In the fireball model[1] (Figure 1a) it is assumed that the overlapping volumes of the two nuclei undergo a completely unelastic collision. The kinetic energy is transformed to internal excitation and a hot gas of nucleous is formed. In the hydrodynamic description[2], the projectile approaches the target, building up pressure in the interaction region bouncing off at an angle and leaving behind an intermediate velocity region resembling a fireball and an excited target remnant (Figure 1b).

In both models, an obvious property of this intermediate region is its disassembly into pions nucleons, and light nuclei. In a thermodynamic model[3], the temperature and relative abundances of the emitted fragments, will vary smoothly with incident energy. On the other hand, a hydrodynamical description[4] of the intermediate region leads to a discontinuity in the temperature and a sudden increase in the production of nucleons relative to light nuclei at a temperature termed the "flash temperature".

The incident energy range of interest for these studies reaches from 10 MeV/nucleon up to 2 GeV/nucleon. This range spans energies just above the coulomb barrier, velocities near the fermi velocity, up to energies where pion production begins to dominate. A gap in the experimental data exists between the highest energies of small cyclotrons ($\sim$20 MeV/nucleon) and the lowest energies at the Bevalac ($\sim$250 MeV/nucleon). This region is now being studied at the CERN Synchrocyclotron (SC) and at the Bevalac. In the near future results in this range will become available from the Superconducting Cyclotron at MSU and from GANIL. We attempted to fill the gap by performing measurements at 100 and 156 MeV/nucleon. Ordinarily, symetric systems would be studied for these effects but a comprehensive set of data over a wide energy range is available only for ^{16}O and ^{20}Ne induced reactions on heavy targets (A $\sim$ 200).

The data that will be considered here are double differential cross section for p, d, t, ^{3}He, and ^{4}He resulting from the systems ^{16}O + Au at 9, 13 and 20 MeV/nucleon[5] ^{20}Ne + Ta at 42 MeV/nucleon,[6] ^{20}Ne + Au at 100 and 150 MeV/nucleon[7], 241 and 393 MeV/nucleon[8] ^{20}Ne + U, and ^{20}Ne + Pb at 800 MeV/nucleon[9]. In order to isolate the component of the measured spectra that can be associated with an intermediate velocity source, one can envision what the fireball model qualitatively predicts for the proton spectra resulting from ^{20}Ne + Au at 150 MeV/nucleon as

Contribution to the Proceedings of the
Relativistic Heavy Ion Winter School, Banff, Alberta, Canada

WHAT CAN WE LEARN FROM INCLUSIVE REACTIONS?

Gary D. Westfall
National Superconducting Cyclotron Laboratory
Michigan State University
E. Lansing, MI 48824

The bulk of experimental results in relativistic heavy ion collisions has been measured in the form of single particle inclusive experiments. In these experiments, only one particle is observed from each reaction while up to 200 particles go undetected. Thus features may emerge that are the result of averaging over many collisions of different characters rather than being indicative of the reaction mechanism. In spite of these limitations, inclusive measurements have told us a great deal about high energy nucleus-nucleus interactions and will continue to provide new information in the future.

Inclusive measurements have several advantages over multi-particle inclusive measurements. One does not introduce an unknown trigger bias in inclusive measurements. The experiments are relatively easy to instrument and carry out. The interpretation of the results is relatively straight-forward in that one has to integrate over all impact parameters. The disadvantages of inclusive data arise from this impact parameter average. A result of the work in the past five years is that almost all models agree with the inclusive data in spite of radically different assumptions. Inclusive reactions are also non-specific. One has to observe all classes of reactions in an attempt to study a given specific aspect of these reactions.

Inclusive measurements subdivide naturally into two distinct areas: light particle emission and projectile/target fragmentation. Fragmentation processes are relatively gentle reactions where large portions of the projectile and target nuclei remain after the collision and are associated with peripheral collisions. To study target fragmentation, techniques such as radiochemical separation and counter experiments using thin targets and detectors designed to handle the very low energy fragments must be used. The analogous phenomena can be studied more easily using projectile breakup because the fragments are moving near the projectile velocity.

Projectile-like fragment inclusive measurements have the advantage that they average over fewer unseen particles. There is a large gap in the measurements performed from 200 to 1000 MeV/nucleon incident energy which leaves a large region to be explored. The fragmentation